Mathematisches Forschungsinstitut Oberwolfach

Model Hierarchies in Atmosphere, Ocean, and Climate Sciences

Organized by
Paola Cessi, San Diego
Rupert Klein, Berlin
Sam Stechmann, Madison
Bjorn Stevens, Hamburg

30 June – 5 July 2024

ABSTRACT. This Oberwolfach workshop was dedicated to continuing the sequence on "Atmosphere-Ocean Science" from (2002, 2006, 2010). The spirit of these events is that of an open invitation to engage in an eye-level exchange on recent developments and pressing challenges in each of the participating disciplines, and to explore possible new routes of interdisciplinary cooperation. This workshop emphasized "model hierarchies" and their importance for the systematic development of both theoretical understanding and methods of scientific investigation. To limit its scope, the workshop focused on (i) scale interactions in the atmosphere and oceans, (ii) thermodynamics and multiphase processes, and (iii) tropical-extratropical interactions from the applied perspective. From a mathematics perspective, challenging aspects of the derivation, justification, and numerical integration of hierarchical reduced models were addressed. Moreover, the workshop explored the potential applicability in atmosphere-ocean science of exciting recent results of mathematical fluid dynamics on "rough path" stochastic modelling and "wild" weak solutions of the Euler and Navier-Stokes equations.

Introduction by the Organizers

The first section of Isaac Held's seminal paper [1] on "The Gap between Simulation and Understanding in Climate Modeling" is entitled "The need for model hierarchies". The author points out that, on the one hand, complex computer simulation models of the atmosphere-ocean system yield highly valuable information in practice. On the other hand, owing to their ever increasing complexity, they do not *per se* foster our understanding of the system's important processes. In contrast, Held states, understanding comes from breaking complexity down into reduced or simplified descriptions of particular processes that involve a manageable number of fundamental concepts. This reduction in complexity allows us to identify the principal causal interactions among them. Such reduced models are traditionally formed in one of two ways: by reducing the complexity of the equations being solved, for instance to isolate interactions operative on particular time or space scales; or by reducing the complexity of the systems being solved, e.g., by introducing symmetries not present in the real world. Such simplifications give rise to model hierarchies on which, as Held concludes, we ought "to base our understanding, describing how the dynamics change as key sources of complexity are added or subtracted. Our understanding benefits from appreciation of the interrelationships among all elements of the hierarchy".

The development of model hierarchies, the study of their individual members, and the synthesis of the insights gained in the process constitutes an ambitious and inherently interdisciplinary research program: Clearly researchers in atmosphere-ocean science know best what are the most important phenomena to be understood next, the most pressing theoretical questions, or what are the most severe current limitations of weather forecasting and climate simulation codes. The design of reduced models, which would help capturing the essence of any of these open questions and their expression in the context of simplified problems, benefits from close cooperation of theorists from the applied side and applied mathematicians. The latter, in particular, contribute their sophisticated model reduction toolkit. Activities of this kind provide for a rich portfolio of serious mathematical questions in PDEs, stochastics, numerical analysis, and scientific computing. The resolution of these questions will primarily be in the hands of mathematicians but they also contribute strongly to atmosphere-ocean science by rigorously consolidating the basis on which its model hierarchy is built.

An interesting mathematical question in this context concerns, for instance, the regime of validity of a given reduced dynamical model. Thus, once the convergence of full-model solutions to those of a reduced model in the appropriate limit is established, the practitioner will also ask how close to the limit we should be for the reduced model to still provide relevant information. For example, Stommel's idealized model for multiple equilibria in ocean flows with heat and salinity [2], or the anelastic [3] and pseudo-incompressible [4] models for atmospheric flows were found to have a broader range of practical validity than that suggested by their derivations, see [5, 6], respectively. In contrast, the classical quasi-geostrophic

theory, see, e.g., [7] requires a non-trivial extension in order to capture some practically important weather regimes [8].

The validity of any practically useful model of geophysical flows based on PDEs is challenged by issues of under-resolution. Practical usefulness implies that processes acting on scales smaller than a certain threshold are represented by some effective parameterizations. Typical examples concern the net effects of turbulence or those of cloud micro-physics on overall cloud dynamics. As a consequence, any exact or numerical approximate solution of these models generally exhibits fluctuations all the way down to the smallest scales, be they defined by the principal design of the model or by the grid resolution in a numerical simulation. This again raises an avalanche of serious mathematical questions: Do rigorous justifications of reduced models allow for solutions spaces that include roughness near the limiting small scales? Are numerical methods used in simulations sufficiently robust under grid-scale perturbations? If one resorts to stochastic modelling to represent the effects of unresolved scales, what are appropriate mathematical structures to bring in the probabilistic effects? Should randomness be added through additional source terms involving additive or multiplicative noise, or should one rather think of stochastic components of flux fields as in fluctuating hydrodynamics [9] and in recent suggestions by D. Holm and colleagues [10]? Is it sufficient to consider the usual white noise–Brownian motion ansatz for stochastic effects in continuum mechanics, or do the nonlinearity and space-time extent of the underlying processes call for advanced concepts such as rough paths, or regularity structures and para-controlled distributions [11, 12, 13, 14]? And finally, are the recently discovered "wild weak solutions" to the Euler and Navier-Stokes equations [15, 16] abstract artefacts that allow mathematicians to better understand intricate properties of the class of weak solutions to the fluid equations, or does the involved convex integration procedure open new avenues to the theoretical description of unresolved scale processes?

This introduction has been adapted from the original Oberwolfach workshop proposal. The organizers hope that the workshop has delivered on their promises, and that the present workshop report will allow the interested reader to get a head-start into the exciting scientific enterprise of "Model Hierarchies in Atmosphere, Ocean, and Climate Sciences".

Paola Cessi, Rupert Klein, Sam Stechmann, and Bjorn Stevens

References

[1] I. M. Held. The gap between simulation and understanding in climate modeling. *Bull. Amer. Meteorol. Soc.*, 86:1609–1614, 2005.

[2] Henry Stommel. Thermohaline convection with two stable regimes of flow. *Tellus*, 13:224–230, 1961.

[3] F. Lipps and R. Hemler. A scale analysis of deep moist convection and some related numerical calculations. *J. Atmos. Sci.*, 39:2192–2210, 1982.

[4] D. R. Durran. Improving the anelastic approximation. *Journal of Atmosphere Sciences*, 46: 1453–1461, 1989.

 [5] Paola Cessi and W. R. Young. Multiple equilibria in two-dimensional thermohaline circula-
     tion. *J. Fluid Mech.*, 241:291–309, 1992.
 [6] R. Klein, U. Achatz, D. Bresch, O. M. Knio, and P. K. Smolarkiewicz. Regime of Validity
     of Sound-Proof Atmospheric Flow Models. *J. Atmos. Sci.*, 67:3226–3237, 2010.
 [7] J. Pedlosky. *Geophysical Fluid Dynamics*. Springer, Berlin, Heidelberg, New York, 2 edition,
     1992.
 [8] R. Klein, L. Schielicke, S. Pfahl, and B. Khouider. QG-DL-Ekman: Dynamics of a diabatic
     layer in the quasi-geostrophic framework. *J. Atmos. Sci.*, 79(3):887–905, 2022.
 [9] L. D. Landau and E. M. Lifshitz. *Fluid Mechanics, Course of Theoretical Physics, Vol. 6*.
     Pergamon Press, 1959.
[10] Holm DD, Cotter CJ, Gottwald GA. Stochastic partial differential fluid equations as a diffu-
     sive limit of deterministic Lagrangian multi-time dynamics. *Proc. R. Soc. A*, 473:20170388,
     2017.
[11] Martin Hairer. A theory of regularity structures. *Invent. Math.*, 198(2):269–504, 2014.
[12] Massimiliano Gubinelli, Peter Imkeller, and Nicolas Perkowski. Paracontrolled distributions
     and singular PDEs. *Forum of Mathematics, Pi*, 3(6), 2015.
[13] D. Breit, E. Feireisl, and M. Hofmanová. *Stochastically Forced Compressible Fluid Flows*.
     de Gruyter, 2018.
[14] C. Bellingeri, A. Djurdjevac, P. K. Friz, and N. Tapia. Transport and continuity equations
     with (very) rough noise. *Partial Differential Equations and Applications*, 2(4):49, 2021.
[15] Camillo De Lellis and László Székelyhidi. Dissipative continuous Euler flows. *Invent. Math.*,
     193:377–407, 2012.
[16] Tristan Buckmaster and Vlad Vicol. Nonuniqueness of weak solutions to the Navier-Stokes
     equation. *Ann. of Math.*, 189:101–144, 2019.

Workshop: Model Hierarchies in Atmosphere, Ocean, and Climate Sciences

Table of Contents

Abstracts

A simple model linking radiative-convective instability, convective aggregation and large-scale dynamics

Peter Haynes

(joint work with Matthew Davison)

Coupling between dynamics and moisture (the dynamics affects the distribution of moisture, the moisture affects latent and radiative heating that drives the dynamics) is a key aspect of the physics of the tropical atmosphere. Two topics that continue to attract significant attention are *convective aggregation* [1], identified as a behaviour in numerical simulations in convection-representing models , and the *Madden-Julian Oscillation* (hereafter MJO) [2], identified in observations as a dominant mode of intraseasonal (1-3 month) variability of the real tropical atmosphere. Convective aggregation is a pattern of behaviour of a modelled tropical atmosphere in which there is no imposed spatial inhomogeneity, but which exhibits spontaneous organisation into regions of two types, one with active convection and large-scale ascent, and the other with convection suppressed by large-scale subsidence, with typical length scales of 100s km. The MJO is typified by growth of a large-scale (several 1000 km) region of convection in the Indian Ocean, which then propagates to the east, at a speed of about 5 ms^{-1}, into the Western Pacific and then decays.

My talk introduced a simple mathematical model to analyse the relation between the phenomenon of convective aggregation and larger scale variability, including MJO-like behaviour, that results from coupling between dynamics and moisture in the tropical atmosphere. The model is based on the single-layer dynamical equations coupled to a moisture field to represent the effects of latent heating and radiative heating. The moisture variable evolves through the effect of precipitation, horizontal convergence, nonlinear horizontal advection and diffusion. Under the *weak temperature gradient approximation* (WTG) the equations may be reduced to a reaction-diffusion equation for moisture, with the 'reaction' term determined by a combination of precipitation and heating. Under certain conditions on the latter the system exhibits bistability, with a horizontally homogeneous state unstable to inhomogeneous disturbances and, as a result, localised regions evolving towards either dry or moist states, with respectively divergence or convergence in the horizontal flow. These regions undergo a *coarsening* process in which length scales systematically increase. A similar reaction-diffusion equation for moisture has been derived under different physical assumptions [3, 4], and coarsening interpreted in such a model as a representation of convective aggregation. In the simplest case coarsening proceeds to the domain scale. When thermal and frictional damping and f-plane rotation are included in the single-layer dynamics, there is a length scale L_{dyn} that sets an upper limit for the applicability of WTG and for the coarsening. The f-plane results provide a basis for interpreting the behaviour of the system on an equatorial β-plane, where the dynamics

allows coherent equatorially confined zonally propagating disturbances, comprising separate moist and dry regions. The key overall properties of the propagating disturbances, the spatial scale and the phase speed, depend on nonlinearity in the coupling between moisture and dynamics. The details of the model and the resulting behaviour are described in [5].

With the model as described above the zonally propagating disturbances are not 'MJO-like'. However when the further ingredients, suggested in previous work to be important aspects of the mechanism for the MJO, of moistening by boundary layer convergence [6] and of the effects of latitudinal moisture gradients [7] , are included in the model, the disturbances become more MJO-like in that phase speeds characteristic of the MJO can be obtained and structures slope westward as latitude increases in each hemisphere. (See Figure 1.)
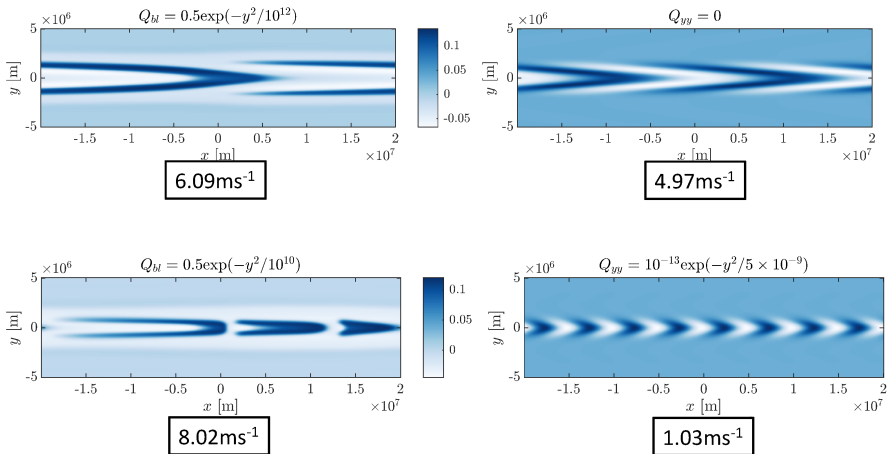
FIGURE 1. Moisture distributions in propagating disturbances when boundary-layer moistening (assuming boundary-layer moisture Q_{bl}) and latitudinal gradients of moisture (assuming second latitudinal derivative Q_{yy}) are included in the model. The left-hand panels show steadily propagating finite-amplitude disturbances. The right-hand panels show the form of the most unstable modes according to linear stability theory. Corresponding phase speeds are given in the boxes.

The model described here, in which the moisture and dynamical fields vary in two spatial dimensions and important aspects of nonlinearity are captured, provides an intermediate model between theoretical models based on linearisation and one spatial dimension and GCMs or convection-resolving models. Future work will investigate the relevance of the model to the horizontal structures of convective aggregation as domain size increases [8] and to the excitation of large-scale convectively coupled waves [9].

REFERENCES

[1] C. Muller, D. Yang, G. Craig, T. Cronin, B. Fildier, J.O. Haerter, C. Hohenegger, B. Mapes, D. Randall, S. Shamekh and S.C. Sherwood, *Spontaneous Aggregation of Convective Storms*, Annual Review of Fluid Mechanics **54** (2022), 133–157, https://doi.org/10.1146/annurev-fluid-022421-011319.

[2] X. Jiang, A.F. Adames, D. Kim, E.D. Maloney, H. Lin, H. Kim, C. Zhang, C.A. DeMott and N.P. Klingaman, *Fifty Years of Research on the Madden-Julian Oscillation: Recent Progress, Challenges, and Perspectives*, Journal of Geophysical Research: Atmospheres **125** (2020), 1–64, https://doi.org/10.1029/2019JD030911.

[3] G.C. Craig and J.M. Mack, *A coarsening model for self-organization of tropical convection*, Journal of Geophysical Research: Atmospheres **118** (2013), 8761–8769, https://doi.org/10.1002/jgrd.50674.

[4] J.M. Windmiller and G.C. Craig, *Universality in the spatial evolution of self-aggregation of tropical convection*, Journal of the Atmospheric Sciences **76** (2019), 1677–1696, https://doi.org/10.1175/JAS-D-18-0129.1.

[5] M. Davison and P. Haynes, *A simple dynamical model linking radiative-convective instability, convective aggregation and large-scale dynamics*, EGUsphere [preprint] (2024), https://doi.org/10.5194/egusphere-2024-206.

[6] A.F. Adames and J.M. Wallace, *Three-dimensional structure and evolution of the vertical velocity and divergence fields in the MJO*, Journal of the Atmospheric Sciences **71** (2014), 4661–4681, https://doi.org/10.1175/JAS-D-14-0091.1.

[7] A.F. Adames and D. Kim, *The MJO as a dispersive, convectively coupled moisture wave: Theory and observations*, Journal of the Atmospheric Sciences, **73** (2016), 913–941, https://doi.org/10.1175/JAS-D-15-0170.1.

[8] T. Yanase, S. Nishizawa, H. Miura and H. Tomita, *Characteristic Form and Distance in High-Level Hierarchical Structure of Self-Aggregated Clouds in Radiative-Convective Equilibrium*, Geophysical Research Letters, **49** (2022), e2022GL100 000,https://doi.org/10.1029/2022GL100000.

[9] J.D. Carstens and A.A. Wing, *Regimes of Convective Self-Aggregation in Convection-Permitting Beta-Plane Simulations*, Journal of the Atmospheric Sciences **80** (2023), https://doi.org/https://doi.org/10.1175/JAS-D-22-0222.1.

Mechanisms of Intertropical Convergence Zone (ITCZ) Edge Intensification: Insight from Idealised Models

MARTIN S. SINGH

(joint work with Julia M. Windmiller)

Recent observational campaigns have revealed that the Atlantic Intertropical Convergence Zone (ITCZ) is often characterised by two separate convergence lines that produce enhanced precipitation at its northern and southern edges [1]. The causes of this "edge-intensification" remain relatively unexplored in the literature, but a similar enhancement of precipitation is observed at the tropical "moist margin", defined by a contour of vertically-integrated column moisture [2], raising the possibility that edge-intensification is a general property of tropical precipitation belts.

Here, we use convection permitting simulations of an idealised overturning circulation to investigate the mechanisms producing edge-intensification in a mock-Walker cell framework. The simulations are performed in a non-rotating channel

domain of length 10 thousand kilometres with an imposed sinusoidal SST pattern driving a large-scale overturning. Consistent with observational analyses, the extent of edge intensification is sensitive to the vertical profile of ascent, which is varied here by controlling the imposed radiative cooling profile. We perform simulations with radiative cooling that peaks either in the lower troposphere ("bottom-heavy cooling"), which results in strong ascending motion in the lower troposphere, or with radiative cooling that peaks in the upper troposphere ("top-heavy cooling"), which results in weaker ascending motion in the lower troposphere. The top-heavy cooling simulation produces a single peak in the mean precipitation rate, while the bottom-heavy simulation produces two peaks (Fig. 1).

We investigate the causes of this "edge intensification" of the precipitation band using mechanism denial experiments applied to the bottom-heavy case. Specifically, we turn off cold pools in the model by disallowing evaporation of rain in the lowest 2 km of the model domain. This results in even stronger edge intensification of precipitation, demonstrating that cold pools are not responsible for the edge intensification. Secondly, we remove the effect of wind speed differences on surface fluxes by homogenising the surface wind that is used to calculate surface enthalpy fluxes. In this case, the precipitation peaks in the centre of the domain, demonstrating that the coupling between surface winds and surface fluxes are key to edge intensification.

The previous results suggest that the strong coupling between surface winds and the large-scale circulation that is present when ascent is concentrated near the surface is the reason that the bottom-heavy case results in edge intensification. Observational studies have also found that the ITCZ itends to be edge intensified when its associated ascent is bottom heavy [2]. Our results provide preliminary evidence that a bottom-heavy ascent profile may *cause* edge intensification.

There are a number of open questions which we intend to pursue in future research. These include:

(1) What sets the distance between convergence lines in the edge-intensified case. Further simulations indicate that the separation distance and number of convergence lines is sensitive to the sea-surface temperature profile imposed. Even with no sea-surface temperature gradient imposed, convergence lines form (as in the well-known phemomenon of convective aggregation), and we are working on a theory for their separation distance.

(2) What is the precise mechanism that results in convection not occurring over the highest sea-surface temperature; can we develop a model that predicts the occurrence of edge intensification?

(3) How are our results affected by rotation?

REFERENCES

[1] J. M. Windmiller & B. Stevens, The inner life of the Atlantic Intertropical Convergence Zone, *Quarterly Journal of the Royal Meteorological Society*, **150** (2023), 523–543.
[2] H. Masunaga, The edge intensification of Eastern Pacific ITCZ convection, *Journal of Climate*, **36** (2023), 3469–3480.
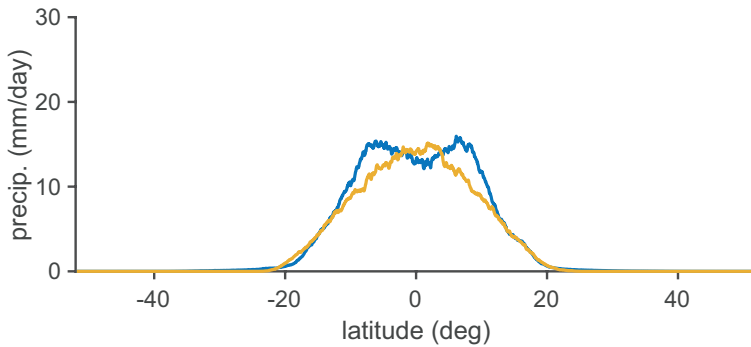
FIGURE 1. Time- and zonal-mean precipitation rate for simulations with (blue) bottom-heavy and (yellow) top-heavy imposed radiative cooling profiles.

Fast jet stream winds get faster under climate change

TIFFANY A. SHAW

(joint work with Osamu Miyawaki)

Earth's upper-level jet streams influence the speed and direction of travel of weather systems and commercial aircraft, and are linked to severe weather occurrence. Climate change is projected to accelerate the average upper-level jet stream winds. However, little is known about how fast (> 99th percentile) upper-level jet stream winds will change. Here we show that fast upper-level jet stream winds get faster under climate change using daily data from climate model projections across a hierarchy of physical complexity. Fast winds also increase ~ 2.5 times more than the average wind response. We show that the multiplicative increase underlying the fast-get-faster response follows from the nonlinear Clausius–Clapeyron relation (moist-get-moister response). The signal is projected to emerge in both hemispheres by 2050 when considering scenario uncertainty. The results can be used to explain projected changes in commercial flight times, record-breaking winds, clear-air turbulence and a potential increase in severe weather occurrence under climate change.

Revitalizing climate science's standard approach

TIFFANY A. SHAW

(joint work with Bjorn Stevens)

The climate science consensus is the physical basis of signals we expect of a warming Earth. Many signals have been successfully predicted. As the Earth warms more and more discrepancies between the real world and our expectations are accumulating. At the same time computational approaches are forgoing standard

assumptions and hierarchical ideas. Taken together the weight of observation and computation is disrupting the unity of ideas and assumptions that underlie the consensus encompassed by theory and numerical climate prediction. Here we review this unity of ideas and assumptions referred to as the standard approach of climate science along with disruptions that have emerged in recent years. Optimally benefiting from the disruptions involves revitalizing elements that have become disconnected as the approach has matured. This includes using signals to our advantage, testing physical hypotheses, determining what we should be able to explain and expect on what timescale and revitalizing the hierarchy.

Glacial Abrupt Climate Change as a Multiscale Phenomenon Resulting from Monostable Excitable Dynamics
Georg Gottwald

Paleoclimate proxies reveal abrupt transitions of the North Atlantic climate during past glacial intervals known as Dansgaard-Oeschger (DO) events. A central feature of DO events is a sudden warming of about $10°C$ in Greenland marking the beginning relatively mild phases termed interstadials. These exhibit gradual cooling over several hundred to a few thousand years until a final abrupt decline brings the temperatures back to cold stadial levels. As of now, the exact mechanism behind this millennial-scale variability remains inconclusive. We aim at providing a dynamically consistent mechanism which gives rise to such abrupt climate changes without invoking any external drivers such as freshwater hosing.

Using the framework of statistical limit laws of deterministic slow-fast chaotic systems, we propose a multiscale setting which deterministically generates alpha-stable noise. This is possible if either a fast process is intermittent with long laminar durations or sporadically exhibits unconstrained large peaks. We illustrate the rigorous theory behind these statistical limit laws in simple examples and then use them to develop conceptual models for DO events.

In the first model abrupt climate changes emerge in a dynamic self-consistent way through complex interactions of a slow ocean, a fast atmosphere and an intermittent process sea-ice process on an intermediate timescale. The abrupt climate changes are caused in our model by intermittencies in the sea-ice cover. The ocean is represented by a Stommel two-box model, the atmosphere by a Lorenz-84 model and the sea-ice cover by a deterministic approximation of correlated additive and multiplicative noise (CAM) process. The key dynamical ingredients of the model are given by stochastic limits of deterministic multi-scale systems and recent results in deterministic homogenisation theory. The deterministic model reproduces statistical features of actual ice-core data such as non-Gaussian α-stable behaviour. The proposed mechanism for abrupt millenial-scale climate change only relies on the existence of a quantity, which exhibits intermittent dynamics on an intermediate time scale. We consider as a particular mechanism intermittent sea-ice cover where the intermittency is generated by emergent atmospheric noise. However,

other mechanisms such as freshwater influxes may also be formulated within the proposed framework. This is work presented in [1].

Whereas this simple model reproduces many statistical features of DO events it fails to reproduce the slow relaxation to the stadia state. We then set out to describe a refined model which better models the heat exchange between the ocean and the atmosphere which is impeded by the presence of an isolating seance cover. In particular, we propose an excitable model to explain Dansgaard-Oeschger cycles, where interstadials occur as noise-induced state space excursions. Our model comprises the mutual multi-scale interactions between four dynamical variables representing Arctic atmospheric temperatures, Nordic Seas' temperatures and sea ice cover, and the Atlantic Meridional Overturning Circulation. The model's atmosphere-ocean heat flux is moderated by the sea ice, which in turn is subject to large perturbations dynamically generated by fast evolving intermittent noise. If supercritical, perturbations trigger interstadial-like state space excursions during which all four model variables undergo qualitative changes that consistently resemble the signature of interstadials in corresponding proxy records. As a physical intermittent process generating the noise we propose convective events in the ocean or atmospheric blocking events. Our model accurately reproduces the DO cycle shape, return times and the dependence of the interstadial and stadial durations on the background conditions. In contrast to the prevailing understanding that DO variability is based on bistability in the underlying dynamics, we show that multi-scale, monostable excitable dynamics provides a promising alternative to explain millennial-scale climate variability associated with DO events. This work appeared in [2].

We discuss how the occurrence of intermittency and/or sporadic large events in a multi-scale setting can serve as a generic dynamical mechanism to generate jump-like behaviour.

References

[1] G. Gottwald, A model for Dansgaard-Oeschger events and millennial-scale abrupt climate change without external forcing, *Climate Dynamics*, **56** (2021), 227–243.
[2] K. Riechers, N. Boers & G. Gottwald, Glacial abrupt climate change as a multi-scale phenomenon resulting from monostable excitable dynamics, *Journal of Climate*, **37**(8) (2024), 2741–2763.

Suppressing cold air events in warm climates: past and future
Eli Tziperman

Wintertime cold air outbreaks are periods of extreme cold, often persisting for several days and spanning hundreds of kilometers or more. They are commonly associated with intrusions of cold polar air into the midlatitudes, but it is unclear whether the air mass's initial temperature in the Arctic or its cooling as it travels is the determining factor in producing a cold air outbreak.

By calculating air parcel trajectories for a pre-industrial climate model scenario, we study the role of the origin and evolution of air masses traveling over sea ice and

land and resulting in wintertime cold air outbreaks over central North America. We find that not all Arctic air masses result in a cold air outbreak when advected into the midlatitudes. We compare trajectories that originate in the Arctic and result in cold air outbreaks to those that also originate in the Arctic but lead to median temperatures when advected into the midlatitudes. While about one-third of the midlatitude temperature difference can be accounted for by the initial height and temperature in the Arctic, the other two-thirds is a result of differences in diabatic heating and cooling as the air masses travel. Vertical mixing of cold surface air into the air mass, while it travels, dominates the diabatic cooling and contributes to the cold events. Air masses leading to cold air outbreaks experience more negative sensible heat flux from the underlying surface, suggesting that pre-conditioning to establish a cold surface is key to producing cold air outbreaks.

In spite of the mean warming trend over the last few decades and its amplification in the Arctic, some studies have found no robust decline or even a slight increase in wintertime cold air outbreaks over North America. But fossil evidence from warmer paleoclimate periods indicates that the interior of North America never dropped below freezing even in the depths of winter, which implies that the maintenance of cold air outbreaks is unlikely to continue indefinitely with future warming. To identify key mechanisms affecting cold air outbreaks and understand how and why they will change in a warmer climate, we examine the development of North American cold air outbreaks in both a pre-industrial and a roughly $8\times CO2$ scenario using the Community Earth System Model, CESM2. We observe a sharp drop-off in the wintertime temperature distribution at the freezing temperature, suppressing below-freezing conditions in the warmer climate and above-freezing conditions in the pre-industrial case. The disappearance of Arctic sea ice and loss of the near-surface temperature inversion dramatically decrease the availability of below-freezing air in source regions. Using an air parcel trajectory analysis, we demonstrate a remarkable similarity in both the dynamics and diabatic effects acting on cold air masses in the two climate scenarios. Diabatic temperature evolution along cold air outbreak trajectories is a competition between cooling from longwave radiation and warming from boundary layer mixing. Surprisingly, while both diabatic effects strengthen in the warmer climate, the balance remains the same, with a net cooling of about -6 K over 10 days.

REFERENCES

[1] Kara Hartig, E. Tziperman, & Chris Loughner, Processes contributing to North American cold air outbreaks based on air parcel trajectory analysis, *Journal of Climate*, **36** (2023), 931–943, doi:10.1175/JCLI-D-22-0204.1
[2] Kara Hartig and E. Tziperman, Suppression of extreme cold weather events in warm climates (2024), submitted.

Nonlinear Coupling Between Slow and Fast Components in Moist Boussinesq Dynamics

Yeyu Zhang

(joint work with Yingshuo Peng, Leslie Smith, Sam Stechmann)

The coupled nonlinear evolution between slow and fast components in geophysical fluid dynamics, including acoustic waves with a small Mach number or inertio-gravity waves with small Froude and Rossby numbers, has been a significant topic of interest for decades. In the moist Boussinesq system, for purely saturated flow with rainfall but no phase changes, it can be shown that the slow modes evolve independently as $\epsilon \to 0$, similar to the dry dynamics [1]. However, phase changes complicate the dynamics by altering buoyancy, which changes its functional form across phase boundaries. Our study develops a fast-wave averaging framework for the moist Boussinesq system [2], extending beyond dry dynamics to include phase transitions between water vapor and liquid water. Analysis of the fast-wave averaging framework [2], the simple ODE model [3], and numerical simulations [4] shows that phase changes cause coupling between slow and fast waves.

The non-dimensional form of the moist Boussinesq model is given by the following equations:

$$(1) \qquad \frac{D\mathbf{u}}{Dt} + \epsilon^{-1}\hat{z} \times \mathbf{u} + \epsilon^{-1}\nabla\phi = \epsilon^{-1}(H_u b_u + H_s b_s)\hat{z}, \quad \nabla \cdot \mathbf{u} = 0,$$

where $\mathbf{u}$ is velocity, ϕ is effective pressure, and $b_u(b_s)$ is buoyancy associated with unsaturated (saturated) region.

$$(2) \qquad \frac{D\theta_e}{Dt} + \epsilon^{-1}w = 0, \quad \frac{Dq_t}{Dt} - \epsilon^{-1}w - \frac{\partial q_r}{\partial z} = 0,$$

where θ_e is equivalent potential temperature, q_t is total water mixing ratio, and q_r is liquid water mixing ratio. The parameters ϵ represent rapid rotation and strong stable stratification, typical of the mid-latitude atmosphere at synoptic scales. $b_u = (\theta_e + (\epsilon - 1)q_t)$, $b_s = (\theta_e - \epsilon q_t)$, and H_u and H_s are Heaviside operators defined as $H_u = 1$ for $q_t < 0$, $H_u = 0$ for $q_t \geq 0$, $H_s = 1 - H_u$. Phase changes affect the system through piecewise linear buoyancy ($b = H_u b_u + H_s b_s$), leading to nonlinear waves near phase interfaces. A model of coupled ordinary differential equations [3] illustrates the nonlinear waves (piecewise sinusoidal functions with different wave frequencies π/N_s and π/N_u in the saturated and unsaturated regions, respectively) that arise in the presence of a phase boundary, as shown in the top panel of Figure 1. These waves have a non-zero time-averaged component, unlike the linear waves in a dry system, which have a time average of zero. This explains the non-zero time-averaged vertical velocity $\langle w \rangle$ and the coupling term $\langle \mathbf{u}_{(W')} \cdot \nabla PV_e \rangle$ in the moist fast-wave averaging framework [2], where PV_e is the equivalent potential temperature (slowly varying component) and the subscript (W') indicates the velocity field from wave components. A suite of numerical simulations [3] is conducted to analyze the coupling term $\langle \mathbf{u}_{(W')} \cdot \nabla PV_e \rangle$, using small values $\epsilon = Fr = Ro = 1, 10^{-1}, 10^{-2}, 10^{-3}$. As shown in the bottom left panel of Figure 1, for $\epsilon = 10^{-1}$ (blue curve), the influence of waves on the slow
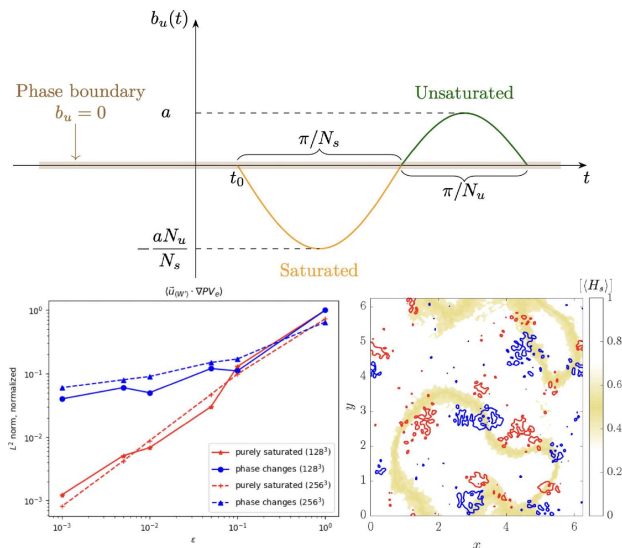
FIGURE 1.

component is relatively small, but does not decrease proportionally with ϵ as it decreases to 10^{-2} and 10^{-3}. This is evident when compared to the benchmark red curve, representing the no phase change case. Additionally, we explore inverse energy transfer to larger scales in strong rotating and stratified flows, considering the effects of water and rapid cloud microphysics [4]. Our findings suggest that the formation of large-scale coherent structures is influenced by nonlinear waves. As shown in the bottom right panel of Figure 1, these nonlinear waves lead to coherent updrafts and downdrafts (red and blue contours) roughly aligned with a slowly varying component of phase boundaries $\langle H_s \rangle$ (yellow bands). This suggests that the slow component is coupled to non-zero time averages of nonlinear waves $(\langle w \rangle)$, indicating slow-fast coupling in moist Boussinesq dynamics with phase changes.

REFERENCES

[1] A.J. Majda & P. Embid *Averaging over fast gravity waves for geophysical flows with unbalanced initial data*, Theoretical and Computational Fluid Dynamics **11** (1998), 155–169.
[2] Zhang, Yeyu, Smith, Leslie M & Stechmann, Samuel N *Fast-wave averaging with phase changes: Asymptotics and application to moist atmospheric dynamics*, Journal of Nonlinear Science **31** (2021), 1–46.
[3] Zhang, Yeyu, Smith, Leslie M & Stechmann, Samuel N, *Effects of clouds and phase changes on fast-wave averaging: a numerical assessment*, Journal of Fluid Mechanics **920** (2021), A49.
[4] Zhang, Yeyu, Peng, Yingshuo & Smith, Leslie M *Inverse Transfer and Coherence in Rotating Stratified Turbulence with Clouds and Phase Transitions*, Submitted.

Do atmospheric models need a partial differential equation for the number of ice particles?

AXEL SEIFERT

Ice clouds are crucial for the radiation budget and precipitation formation. Nevertheless, many atmospheric models predict only the bulk ice water content but not the number of ice particles. By doing so, they miss two important aspects of clouds. Firstly, water vapor and ice are rarely in thermodynamic equilibrium in the atmosphere. They form a metastable system that allows for high ice supersaturation and hysteresis. To describe this nonlinear system, ice water content alone is not enough. The phase relaxation time depends primarily on particle size and number, and therefore the number of ice particles is needed to describe non-equilibrium behavior correctly [1]. Forecasting ice supersaturation, on the other hand, is a prerequisite to predicting the formation of contrails. Long-lived contrails form only in ice supersaturated regions and are important for the non-CO2 climate effect of aviation. Secondly, ice clouds form mostly through heterogeneous ice nucleation. Thus, the microphysical and radiative properties of ice clouds depend on the number of available aerosol or ice nucleating particles. For example, Saharan dust can affect the properties of cirrus clouds associated with synoptic-scale storms and greatly modify radiative fluxes and surface temperature. Introducing only the additional equation for the number of ice particles the global ICON model can describe most of this sensitivity due to Saharan dust. This improves the forecasts of solar irradiance at the surface during Saharan dust events. A precise day-ahead estimate of solar irradiance and, thus, photovoltaic power is crucial for the renewable energy market. Hence, introducing the number of ice particles as an additional equation seems worthwhile. Interestingly, a sub-grid sensitivity remains, which needs to be described by an additional parameterization of 'dust cirrus' [2] . To understand the time evolution of ice crystal number due to aggregation and other sources and sinks, a hierarchy of microphysical models is applied. The geometry of aggregate snowflakes can be studied using an aggregation model that simulates the growth of individual snowflakes [3]. The growth of ice particles by depositional growth, aggregation, and riming can be investigated using Monte-Carlo super-particle models [4, 5], which explicitly simulate the evolution of the particle size distribution in a multi-dimensional phase space. Finally, machine learning methods can be helpful to perform the coarse-graining to the desired ODE system which can then be applied in weather and climate models [6, 7].

REFERENCES

[1] Köhler, C., and Seifert, A. (2015). Identifying sensitivities for cirrus modelling using a two-moment two-mode bulk microphysics scheme. Tellus B, 67(1), 24494.

[2] Seifert, A., et al. (2023). Aerosol-cloud-radiation interaction during Saharan dust episodes: the dusty cirrus puzzle, Atmos. Chem. Phys., 23, 6409–6430, https://doi.org/10.5194/acp-23-6409-2023, 2023.

[3] Karrer, M., Seifert, A., Siewert, C., Ori, D., von Lerber, A., and Kneifel, S. (2020). Ice particle properties inferred from aggregation modeling. Journal of Advances in Modeling Earth Systems, 12, e2020MS002066. https://doi.org/10.1029/2020MS002066

[4] Brdar, S., and Seifert, A. (2018). McSnow: A Monte-Carlo particle model for riming and aggregation of ice particles in a multidimensional microphysical phase space. Journal of Advances in Modeling Earth Systems, 10, 187–206. https://doi.org/10.1002/2017MS001167

[5] Welss, J. N., Siewert, C., and Seifert, A. (2024). Explicit habit-prediction in the Lagrangian super-particle ice microphysics model McSnow. Journal of Advances in Modeling Earth Systems, 16(4), e2023MS003805.

[6] Seifert, A., and Rasp, S. (2020). Potential and limitations of machine learning for modeling warm-rain cloud microphysical processes. Journal of Advances in Modeling Earth Systems, 12(12), e2020MS002301.

[7] Seifert, A., and Siewert, C. (2024). An ML-based P3-like multimodal two-moment ice microphysics in the ICON model. Journal of Advances in Modeling Earth Systems, in press.

A three-scale reduced effective framework for mesoscale cloud patterns

Franziska Glassmeier

(joint work with Benjamin Hernandez, Pouriya Alinaghi, Fredrik Jansson)

Due to their complex multiscale nature, clouds are a major source of uncertainty in climate projections. Our models assume a scale gap between the scales of cloud-formation and large-scale cloud-controlling factors. It is now clear that this assumption does not hold, which explains why cloud-climate uncertainties, especially rapid adjustments to cloud-mediated aerosol forcing and (sub)tropical cloud feedbacks, emerge within the assumed gap. This mesoscale is where cloud fields organize into striking patterns that cover hundreds of kilometers and evolve over hours. We disentangle the mesoscale challenge by distinguishing three scales: large-scale cloud-controlling factors such as sea-surface temperature, microscale processes like rain formation, and the mesoscale self-organization of cloud patterns.

A first promising example for capturing mesoscale self-organization as low-dimensional, emergent behavior includes stratocumulus cloud decks over the subtropical oceans. These cloud decks exhibit bi-stable behavior between a reflective, high-cloud cover *closed-cell state*, and an inverse pattern of an *open-cell state*, characterized by low cloud-cover and reflectivity. A Freidlin–Wentzell quasi-potential suggests that pockets of open cells that can sometimes be observed embedded within predominantly closed-cell decks can be understood as noise-induced transitions.

As second example, fields of shallow cumulus clouds in the trade-wind regions are characterized by variability in their patterns of horizontal arrangement. We explore the nature of such patterns by varying the initial spatial arrangement of a cloud field in large-eddy simulations. Based on this data, we hypothesize that mesoscale organization in these types of clouds may feature a Hopf bifurcation as the cloud-droplet number parameter is varied.

References

[1] F. Glassmeier and G. Feingold, *Network approach to patterns in stratocumulus clouds*, PNAS **114**(40) (2017), 10578—10583.

[2] F. Glassmeier, F. Hoffmann, J. S. Johnson, T. Yamaguchi, K. S. Carslaw and G. Feingold *Aerosol-cloud-climate cooling overestimated by ship-track data*, Science **371** (2021), 485–489.

[3] M. Janssens, J. Vilà-Guerau de Arellano, C. C. van Heerwaarden and S. R. de Roode, A. P. Siebesma and F. Glassmeier *Nonprecipitating Shallow Cumulus Convection Is Intrinsically Unstable to Length Scale Growth*, J. Atmos. Sci. **80**(30) (2023), 849–870.

Lower bounds on irreducible imprecision in the climate system
Bjorn Stevens

It is well established that the equations governing the evolution of earth's atmosphere allow for deterministic predictability of about 2-3 weeks. After that even infinitesimally small differences in initial conditions lead to large differences in predictions - presumably as system trajectories diverge across the attractor. On longer timescales predictability may be maintained for some aspects of the system, but only in a probabilistic sense due to their conditioning by slowly evolving and more inherently predictable components of the system - like the ocean or the soils.

On yet longer timescales the attractor (to the extent one exists) is thought to be shaped by the boundary conditions - pros and cons of land use, greenhouse gases etc., defining an invariant measure that governs the statistics of the system. What is unknown is whether this attractor exists and how stable it is to structural perturbations to the governing equations, for instance as arises from the combination of their discretization and the parameterization of poorly understood subsystems (ecology) or unresolved scales of motion. The extent to which the invariant measure changes due to small changes in the structure of the system limits the probabilistic predictability of the system and raises the question as to whether "better" models make better predictions.

Emergent effective dynamics of warm cloud precipitation
Anna Frishman
(joint work with Shai Kapon and Nadir Jeevanjee)

Cloud observables such as precipitation efficiency and cloud lifetime are key quantities in weather and climate, but understanding their quantitative connection to initial conditions such as initial cloud water mass or droplet size remains challenging. In the talk I presented a hierarchical approach to characterize such observables, using an idealized bin microphysics scheme modeling gravitational coagulation and fallout. In the spirit of previous works [1, 2, 3], we focus on the effective bulk dynamics describing the evolution of total cloud and rain water. In our treatment, we separate the dynamics into a mass-conserving and fallout-dominated regime. To model the accretion of cloud drops by rain drops we use a constant accretion

rate, similarly to previous work [4]. We emphasize that this implies universal normalized dynamics for the rain and cloud mass during the mass conserving stage, and demonstrate this behavior in our cloud simulations. For the fallout-dominated regime, we find that sedimentation can be modeled with a bulk fall speed which is constant in time despite an evolving raindrop distribution. Combining the two regimes reveals that the overall dynamics are governed by a single non-dimensional emergent parameter μ, the ratio between effective accretion and sedimentation time scales. The dependence on a clouds initial conditions, given by the initial drop size distribution, is encoded in these two effective rates, which we infer for each cloud in a vast range of cloud simulations. We find that cloud observables from the simulations, such as cloud lifetimes and the accumulated rain mass, accordingly collapse as a function of μ. We also find an unexpected relationship between cloud water and accumulated rain, which comes out of our bulk modeling.

Beyond our idealized model, our findings could be relevant for part of a clouds life cycle: after some rain drops have formed, in clouds where evaporation and condensation processes (which are not included in our modeling) are well separated in time from accretion and rainfall, e.g. in mildly polluted clouds [5]. At earlier times, during the autoconversion stage when the first few rain drops form, evaporation and entrainment usually determine if the cloud would be able to develop a rain population before dissipating away. Our model is therefore unrealistic in this respect: the autoconversion stage does not play an important role in determining the cloud observables, and we find that most of the clouds mass is converted to rain for all our clouds. This highlights that our work is only the simplest first step, and more realistic models are needed to test its direct applicability. In particular, it would be interesting to use a similar hierarchical approach in a model that includes the clouds full life-cycle: one might then imagine a larger set of effective rates, corresponding to a wider range of temporal regimes and processes. The ratios between these rates would then give the relevant dimensionless parameters determining the average cloud observables. Developing such a framework is an exciting prospect for future work.

REFERENCES

[1] E. Kessler, *On the Distribution and Continuity of Water Substance in Atmospheric Circulations*, pp. 1–84. Boston, MA: American Meteorological Society, 1969.
[2] A. Seifert and K. D. Beheng, "A double-moment parameterization for simulating autoconversion, accretion and selfcollection," *Atmospheric Research*, vol. 59-60, pp. 265–281, Oct. 2001.
[3] A. Khain, K. Beheng, A. Heymsfield, A. Korolev, S. Krichak, Z. Levin, M. Pinsky, V. Phillips, T. Prabhakaran, A. Teller, *et al.*, "Representation of microphysical processes in cloud-resolving models: Spectral (bin) microphysics versus bulk parameterization," *Reviews of Geophysics*, vol. 53, no. 2, pp. 247–322, 2015.
[4] K. Beheng, "A parameterization of warm cloud microphysical conversion processes," *Atmospheric Research*, vol. 33, no. 1, pp. 193–206, 1994. 11th International Conference on Clouds and Precipitation, Part II.
[5] G. Dagan, I. Koren, and O. Altaratz, "Competition between core and periphery-based processes in warm convective clouds – from invigoration to suppression," *Atmospheric Chemistry and Physics*, vol. 15, no. 5, pp. 2749–2760, 2015.

Long-time behavior of the compressible Navier-Stokes-(Fourier) system

EDUARD FEIREISL

(joint work with Agnieszka Świerczewska-Gwiazda)

We review some recent results concerning the long–time behaviour of solutions to the Navier–Stokes–Fourier system describing the motion of a general viscous, compressible and heat conducting fluid:

$$\partial_t \rho + \nabla \cdot (\rho \vec{u}) = 0,$$
$$\partial_t(\rho \vec{u}) + \nabla \cdot (\rho \vec{u} \otimes \vec{u}) + \nabla p(\rho, \theta) = \nabla \cdot \mathbb{S}(\nabla \vec{u}) + \rho \nabla G,$$
$$\partial_t(\rho e(\rho, \theta)) + \nabla(\rho e(\rho, \theta) \vec{u}) + \nabla \cdot \vec{q}(\nabla \theta) = \mathbb{S}(\nabla \vec{u}) : \nabla \vec{u} - p(\rho, \theta) \nabla \cdot \vec{u},$$

where

$$\mathbb{S}(\nabla \vec{u}) = \mu \left(\nabla \vec{+} \nabla^t \vec{u} - \frac{2}{d} \nabla \cdot \vec{u} \mathbb{I} \right) + \eta \nabla \cdot \vec{u} \mathbb{I}, \ \mu > 0, \ \eta \geq 0,$$
$$\vec{q}(\nabla \theta) = -\kappa \nabla \theta, \ \kappa > 0.$$

The problem is considered in a bounded spatial domain $\Omega \subset R^3$, and supplemented with the non–conservative boundary conditions

$$\vec{u}|_{\partial \Omega} = 0, \ \theta|_{\partial \Omega} = \theta_B.$$

An iconic example is the celebrated Rayleigh–Bénard convection problem.

We report the following results concerning existence and long–time behaviour of solutions.

(1) Under suitable constitutive restrictions, the problem admits global in time weak solutions for any finite energy initial data. The class of weak solutions complies with the weak–strong uniqueness principle, see [1], [2].
(2) The problem admits a bounded absorbing set in the trajectory space, meaning the space of entire solutions defined for any time $t \in (-\infty, \infty)$, see [3, Theorem 3.1].
(3) The system admits a compact global attractor in the trajectory space, see [3, Theorem 3.4].

As a direct consequence of the above mentioned results we can also show:

(1) Applying the abstract Krylov–Bogolyubov method, we deduce the existence of stationary statistical solutions, see [3, Theorem 3.4]. More precisely, any ω-limit set in the trajectory space supports a time shift invariant measure.
(2) The time ergodic averages converge a.s. with respect to the invariant measure. This can be seen as a special version of the ergodic theorem valid for the Navier–Stokes–Fourier system.

REFERENCES

[1] N. Chaudhuri and E. Feireisl, *Navier-Stokes-Fourier system with Dirichlet boundary conditions*, Appl. Anal. **101** (2022), 4076–4094
[2] E. Feireisl and A. Novotný, *Mathematics of open fluid systems*, Birkhäuser–Verlag, Basel, 2022
[3] E. Feireisl and A. Świerczewska-Gwiazda, *The Rayleigh-Bénard problem for compressible fluid flows*, Arch. Ration. Mech. Anal. **247**, (2023), Paper No. 9, 31

Generalised Lagrangian mean: theory and numerics

JACQUES VANNESTE

(joint work with Lois Baker, Andrew Gilbert, Hossein Kafiabad, Abhijeet Minz)

Because of their finite resolution, numerical models of the atmosphere and ocean necessarily solve averaged equations, relying on parameterisations of unresolved processes such as small-scale turbulence. Different averaging procedures lead to different averaged models with different unresolved terms to parameterise. Lagrangian averaging, carried out at fixed particle label rather than the fixed position of the traditional Eulerian averaging, is an advantageous procedure in that it preserves the advective structure of the equations governing fluid motion. In principle this simplifies the task of parameterisation.

The generalised Lagrangian mean (GLM) theory of Andrews & McIntyre provides a powerful formulation of Lagrangian averaging [1, 2]. In modern language [3, 4], it can be described as follows. Denote by φ the flow map, such that $x = \varphi(a, t)$ is the position at time t of the fluid particle labelled by a, and by $\bar{\bar{\varphi}}$ the mean flow map (different definitions are possible for $\bar{\bar{\varphi}}$). Writing the flow map as the composition $\varphi = \Xi \circ \bar{\bar{\varphi}}$ of the perturbation map Ξ and mean map, we define the Lagrangian mean of any tensor τ as

$$(1) \qquad \overline{\tau}^{\mathrm{L}} = \overline{\Xi^* \tau},$$

where the overbar denotes averaging and Ξ^* is the pull-back by Ξ.

Lagrangian averaging applies straightforwardly to fluid equations when the advection terms are written in terms of the Lie derivative $\mathcal{L}$. We take the Euler equations for ideal incompressible fluids as a basic example. These equations read

$$(2) \qquad (\partial_t + \mathcal{L}_u)\nu = -d\pi, \quad \operatorname{div} u = 0, \quad \nu = u_\flat.$$

Here $u = \partial_t \varphi \circ \varphi^{-1}$ is the velocity vector, ν its dual 1-form (the momentum, with $\nu = u\,dx + v\,dy + w\,dz$ in Euclidean space and Cartesian coordinates) and $\pi = p - \frac{1}{2}|u|^2$. Applying the pull-back Ξ^* to (2) and averaging leads to

$$(3) \qquad (\partial_t + \mathcal{L}_{\bar{\bar{u}}})\overline{\nu}^{\mathrm{L}} = -d\overline{\pi}^{\mathrm{L}},$$

where $\bar{\bar{u}} = \partial_t \bar{\bar{\varphi}} \circ \bar{\bar{\varphi}}^{-1}$ is the mean velocity and we assume that the average leaves $\bar{\bar{u}}$ unchanged. Eq. (3) is not closed since $\overline{\nu}^{\mathrm{L}}$ is not immediately related to $\bar{\bar{u}}$. The difference $\overline{\nu}^{\mathrm{L}} - \bar{\bar{u}}_\flat$ is (minus) the so-called pseudomomentum. It captures the impact on the mean flow of the fluctuations eliminated by averaging and needs to be parameterised.

A practical form of averaging is time averaging, which filters out fast dynamics such as high-frequency waves. Several specific time averages can be considered. The simplest is the exponential mean which, for a function of time $f(t)$ can be equivalently defined as a convolution or as the solution of a differential equation:

$$(4) \qquad \bar{f}(t) = \alpha \int_{-\infty}^{t} \mathrm{e}^{-\alpha(t-s)} f(s)\, ds \quad \text{or} \quad \dot{\bar{f}} = \alpha(f - \bar{f}),$$

where the parameter $\alpha > 0$ is the inverse of the averaging time scale. In the GLM context [5], we can choose the mean flow map as the component-wise exponential average

$$(5) \qquad \bar{\varphi}^i(a) = \alpha \int_{-\infty}^{t} \mathrm{e}^{-\alpha(t-s)} \varphi^i(a, s)\, ds.$$

The corresponding mean velocity can be shown to be given by

$$(6) \qquad \bar{\bar{u}}(x, t) = \alpha(\Xi(x, t) - x),$$

where the perturbation map Ξ satisfies

$$(7) \qquad \partial_t \Xi + \Xi_* \bar{\bar{u}} = u \circ \Xi.$$

The Lagrangian mean of a tensor field τ is defined by

$$(8) \qquad \bar{\varphi}^* \overline{\tau}^{\mathrm{L}} = \alpha \int_{-\infty}^{t} \mathrm{e}^{\alpha(t-s)} \varphi^* \tau(\cdot, s)\, ds,$$

approximating (1). It satisfies

$$(9) \qquad (\partial_t + \mathcal{L}_{\bar{\bar{u}}}) \overline{\tau}^{\mathrm{L}} = \alpha(\Xi^* \tau - \overline{\tau}^{\mathrm{L}}).$$

We can solve (7)–(9) together with the partial differential equations governing the dynamics of u and τ numerically to compute the Lagrangian mean $\overline{\tau}^{\mathrm{L}}$ on the fly. We applied this approach to simulations of the rotating shallow-water system in which a large-amplitude Poincaré wave is superimposed to a complex turbulent flow. See Ref. [5] for details and Ref. [6] for the implementation of more advanced temporal averages and their use for wave–mean-flow decomposition.

REFERENCES

[1] D. G. Andrews & M. E. McIntyre, *An exact theory of nonlinear waves on a Lagrangian-mean flow*, Journal of Fluid Mechanics **89** (1978), 609–646.

[2] O. Bühler, *Waves and mean flows*, Cambridge University Press, 2nd ed. (2014).

[3] A. D. Gilbert & J. Vanneste, *Geometric generalised Lagrangian-mean theories*, Journal of Fluid Mechanics **839** (2018), 95–134.

[4] A. D. Gilbert & J. Vanneste, *Geometric approaches to Lagrangian averaging*, Annual Review of Fluid Mechanics, in press (arXiv:2405.04394).

[5] A. Minz, L. E. Baker, H. A. Kafiabad & J. Vanneste, *The exponential Lagrangian mean*, preprint (arXiv:2406.18243).

[6] L. E. Baker, H. A. Kafiabad & J. Vanneste, *Lagrangian filtering for wave-mean flow decomposition*, preprint (arXiv:2406.03477).

Semiclassical near-inertial waves

Jörn Callies

(joint work with Scott Conn, Albion Lawrence)

Near-inertial waves often dominate velocities in the upper ocean after being resonantly excited by a passing storm. It is important to understand the evolution of these waves because they (1) can substantially deepen the mixed layer and thus have a large impact on the thermal coupling with the atmosphere, (2) are a key energy source for the internal-wave field in the interior ocean, (3) may extract energy from the mesoscale eddy field, and (4) are important in search and rescue operations.

In much of the world ocean, the evolution of near-inertial waves is strongly modulated by the presence of mesoscale eddies. The wave evolution is typically understood through either of two theories. Kunze [1] assumed a spatial-scale separation between the waves and eddies to derive ray equations that describe the wave propagation through an eddy field. Young and Ben Jelloul [2, YBJ] criticized the spatial-scale separation assumption because the waves are forced by storms that are larger than mesoscale eddies, not smaller. YBJ derived a field equation for the evolution of the wave field, taking advantage of the separation of time scales only.

This presentation has two parts. First, I will demonstrate that the YBJ model can explain the observed evolution of near-inertial waves in the Northeast Atlantic and that this match with observations can be achieved only if the interaction with mesoscale eddies is taken into account. This provides an example of a compressed model hierarchy, in which simple theory directly explains observations of the real ocean. Second, I will clarify the relationship between YBJ's theory and Kunze's ray equations. The YBJ equation describing the evolution of the near-inertial wave field is a Schrödinger equation, and I will show that Kunze's ray equations correspond to the classical limit of weak wave dispersion. This classical limit can be exploited independent of the scale of the atmospheric forcing and offers a post hoc justification for Kunze's scale-separation assumption. I will apply semiclassical analysis to calculate eigenmodes for a set of increasingly complex examples.

References

[1] E. Kunze, *Near-inertial wave propagation in geostrophic shear*, Journal of Physical Oceanography **15** (1985), 544–565.

[2] W. R. Young, M. Ben Jelloul, *Propagation of near-inertial oscillations through a geostrophic flow*, Journal of Marine Research **55** (1997), 735–766.

Modeling a hurricane boundary layer through matched asymptotics

Tom Dörffel

(joint work with Rupert Klein, Boualem Khouider)

Tropical cyclones (TCs) are a multiscale phenomenon that, for a comprehensive understanding, require methods to resolve the processes on the individual scales. Together with my coauthors, I am investigating the scale interaction that determines the dynamics of TCs, particularly the interaction of the bulk vortex with a friction-dominated boundary layer closest to the ocean surface.

Flows in the atmosphere behave according to the dominant balances emerging on different spatiotemporal scales [1]. This idea has been applied to investigate the dynamics of TCs [2, 3]. The authors restricted their analysis to the bulk-flow scaling regime above the boundary layer where the flow is frictionless and balanced. An asymptotically consistent theory to incorporate the effects of a frictional boundary layer is yet missing. Klein et al. [4] developed a theory on the boundary layer beneath a balanced quasi-geostrophic (GQ) flow, which we take as a blueprint to adapt to the case of a TC flow.

Similar to [4], three scaling regimes arise in the case of TCs, of which the friction layer and the bulk flow are already established in the literature [2, 5, 6, 7, among others]. The direct matching of the two regimes leads to inconsistencies, which is why a third, intermediate layer is necessary. The convection-controlling layer (CCL) turns out to play an important role that arises between the two regimes. It acts as a transition regime between the friction layer and the bulk flow, cf. Fig. 1.

The friction layer, as the name suggests, is guided predominantly by frictionally driven convergent motions, where there is no significant contribution of moist convection. In fact, the flow can be considered as dry adiabatic. The characteristic flow pattern consists of an inward-directed flow right above the sea surface. This flow turns over and is injected into the atmosphere above, cf. the lower part of Fig. 1. Mathematically, the friction layer is necessary to meet the semi-slip boundary conditions. Otherwise, these conditions could not be satisfied for the frictionless regime of the bulk flow. The result is a balanced-vortex version of the well-known Ekman pumping, which transports moist air into the atmosphere above.

The bulk, in turn, is characterized by the overturning and outward-directed secondary circulation (cf. the upper part of Fig. 1) that is due to moist convection. Air masses enter from below carrying moist entropy and angular momentum. While the angular momentum is matched to the CCL, the moisture content (more specifically, their convectively available potential energy) determines the trajectory in the r-z plane. Vertical motions are guided by the moist diabatic heat release obeying the weak-temperature gradient approximation. Radial motions follow from mass continuity.

The CCL forms a layer between the friction layer and the bulk flow. From an asymptotic point of view, it allows for potential temperature variations $\Theta^{(3)}$ due to diabatic heat release that are one order in $\varepsilon^{1/2}$ larger than what is allowed in
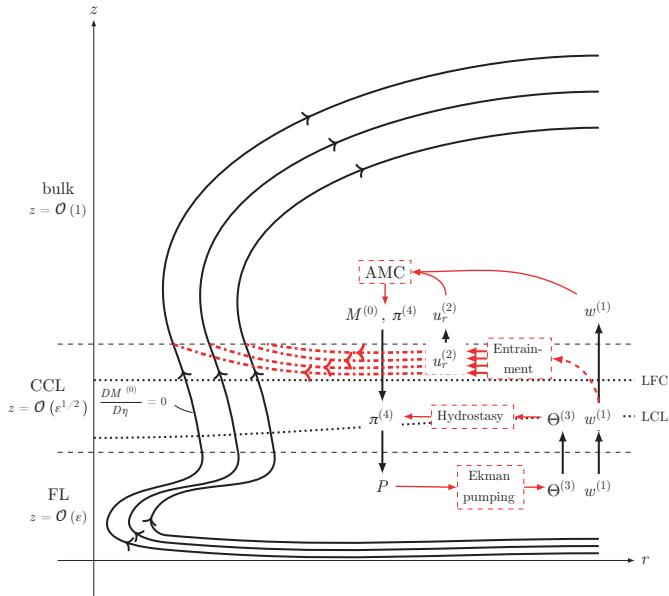
FIGURE 1.   Structure of an axisymmetric tropical cyclone.
Shown is the overturning secondary circulation affected by the
physical properties manifesting in the three scaling regimes. On
the right, the interaction of the physical quantities within each
scaling regime is highlighted. Black arrows indicate the flow of
information subject to the matching conditions. Red arrows are
the input and output of the leading-order governing processes.

the bulk flow. By doing so, it is the CCL where the onsets of moist diabatic heat
release and free convection are located. The thermodynamic adjustments of the
CCL to the forcings of the bulk and friction layer regulate the release of diabatic
heat.

The CCL and the friction layer evolve asymptotically fast, i.e., they adapt im-
mediately to changes that the bulk flow prescribes. It is the angular momentum in
the $z \to 0$ limit that drives the CCL and the friction layer. Angular momentum in
the bulk, however, is conserved and follows the streamlines of the secondary circu-
lation which start at the matching boundary between bulk and CCL. Considering
only that leading-order dynamics, there would be no pathway to intensification
since the controlling angular momentum at the bulk-CCL interface remains sta-
tionary.

The asymptotic analysis revealed that within the CCL there is a route to inten-
sification. At next-to-leading-order, the angular momentum balance is guided by
a second-order contribution to radially converging mass fluxes, depicted as dash-
dotted red arrows in Fig. 1. They allow transporting angular momentum from

larger to smaller radii and with that intensifying the vortex. The systematic approach of asymptotic analysis shows how exactly this next-to-leading order CCL flow enters the picture. It gives rise to the hypothesis that it is entrainment that is responsible for these secondary effects. On the vortex core scale, entraining air is dragged into individual cloud towers once air masses pass the level of free convection. The accumulated effect of the individual cloud towers causes a radial mean flow. This radial mean flow might be what causes the vortex to intensify in the way described above.

The presented work shows the importance of representing entrainment in models of numerical weather prediction in order to capture TC intensification. It remains open, however, to verify the pathway as it was discovered by asymptotic analysis. This will be accomplished by means of three-dimensional and high-resolution simulation data and is subject to future work.

References

[1] R. Klein, *Scale-Dependent Models for Atmospheric Flows*, Annu. Rev. Fluid Mechanics (2010), 42:249–74.
[2] E. Päschke, P. Marschalik, A. Z. Owinoh, and R. Klein, *Motion and structure of atmospheric mesoscale baroclinic vortices: dry air and weak environmental shear*, J. Fluid Mech. (2012), 701:137–170.
[3] T. Dörffel, A. Papke, R. Klein, N. Ernst, and P. K. Smolarkiewicz, *Dynamics of tilted atmospheric vortices under asymmetric diabatic heating*, Theor. Comput. Fluid Dyn. (2021) 35:831–873.
[4] R. Klein, L. Schielicke, S. Pfahl, B. Khouider, *QG-DL-Ekman: Dynamics of a Diabatic Layer in the Quasi-Geostrophic Framework*, J. Atmos. Sci. (2022), 79:887-905.
[5] A. Eliassen, *On the Ekman Layer in a Circular Vortex*, J. Met. Soc. Japan Ser. II (1971), 49A:784–789
[6] K. A. Emanuel, *An Air-Sea Interaction Theory for Tropical Cyclones. Part II: Steady-State Maintenance*, J. Atmos. Sci. (1986), 43:585–605.
[7] R. Rotunno and K. A. Emanuel, *An Air-Sea Interaction Theory for Tropical Cyclones. Part II: Evolutionary Study Using a Nonhydrostatic Axisymmetric Numerical Model*, J. Atmos. Sci. (1987), 44:542–561.

Moisture and Math

SAMUEL STECHMANN

(joint work with Leslie Smith, Parvathi Kooloth, David Marsico, Shukai Du)

Moisture and clouds are some of the most important quantities in weather and climate predictions. Nevertheless, our understanding of moist atmospheric dynamics is much less advanced in comparison to dry atmospheric dynamics. In light of this, I presented some results that aim to advance our theoretical understanding of fundamentals of geophysical fluid dynamics with moisture and clouds. In particular, I presented results on energetics [6], conservation of potential vorticity [4, 5], and the quasi-geostrophic approximation [8, 1]. Also, I briefly described preliminary results (in joint work with David Marsico and Shukai Du) on numerical methods for the partial differential equations (PDEs) for atmospheric dynamics with

moisture and clouds, and the quest to obtain second-order numerical accuracy. The numerical accuracy with clouds is degraded in comparison to numerical accuracy without clouds, and the order of accuracy appears to be different in different norms (e.g., L^2 versus L^∞ norms). Further understanding of regularity of solutions, along the lines of recent PDE analysis results for other moist PDEs [2, 3, 7], could be helpful for designing numerical methods and understanding order of accuracy. Model hierarchies were involved in the presentation in the hierarchy of complexity of moisture and cloud properties, and in the hierarchy of Boussinesq, anelastic, and compressible fluid dynamics equations.

REFERENCES

[1] D. Bäumer, S. Hittmeir, R. Klein, *Scaling approaches to quasigeostrophic theory for moist, precipitating air*, J. Atmos. Sci. **80** (2023), 1771–1786.

[2] S. Hittmeir, R. Klein, J. Li, and E. S. Titi, *Global well-posedness for passively transported nonlinear moisture dynamics with phase changes*, Nonlinearity **30** (2017), 3676–3718.

[3] S. Hittmeir, R. Klein, J. Li, and E. S. Titi, *Global well-posedness for the primitive equations coupled to nonlinear moisture dynamics with phase changes*, Nonlinearity **33** (2020), 3206–3236.

[4] P. Kooloth, L. M. Smith, S. N. Stechmann, *Conservation laws for potential vorticity in a salty ocean or cloudy atmosphere*, Geophys. Res. Lett. **49** (2022), e2022GL100009.

[5] P. Kooloth, L. M. Smith, S. N. Stechmann, *Hamilton's principle with phase changes and conservation principles for moist potential vorticity*, Q. J. Roy. Met. Soc. **149** (2023), 1056–1072.

[6] D. H. Marsico, L. M. Smith, S. N. Stechmann, *Energy decompositions for moist Boussinesq and anelastic equations with phase changes*, J. Atmos. Sci. **76** (2019), 3569–3587.

[7] A. Remond-Tiedrez, L. M. Smith, and S. N. Stechmann, *A nonlinear elliptic PDE from atmospheric science: well-posedness and regularity at cloud edge*, Journal of Mathematical Fluid Mechanics **26** (2024), 30.

[8] L. M. Smith, S. N. Stechmann, *Precipitating quasigeostrophic equations and potential vorticity inversion with phase changes*, J. Atmos. Sci. **74** (2017), 3285–3303.

Entropic optimal transport solutions of the semigeostrophic equations

COLIN COTTER

(joint work with Jean-David Benamou, Hugo Malamut)

Numerical solution of the semigeostrophic equations is useful as a tool for verifying and validating standard numerical approaches to equations with less approximations, in support of atmosphere model development, as well as in designing physics parameterisations. In this work we revisit the "geometric algorithm" developed by Mike Cullen and co-workers, described in [2]. This algorithm works in geostrophic coordinates, obtaining the transformation back to physical coordinates at each step by solving an optimal transport problem. The transport map then defines the vector field describing the instantaneous motion of the fluid particles in geostrophic space. It also defines the reconstruction of the temperature and fluid velocity in the physical domain.

In this work, we replace the solution strategy in the geometric algorithm by introducing an entropic regularisation, making use of the multiscale acceleration to

obtain a fast solver [3]. To provide a bit more detail, here we describe the formulation for the semigeostrophic approximation of the vertical slice incompressible Boussinesq equations with a out of plane constant linear temperature gradient s, written in Lagrangian coordinates,

$$\dot{X}(a,t)U := -f(Z(a,t) - z(X(a,t), Z(a,t)),$$
$$\dot{Z}(a,t)W := f(Z(a,t) - x(X(a,t), Z(a,t)),$$

where X is the horizontal coordinate, and Z is the vertical coordinate, f is the (constant) Coriolis parameter, a is the Lagrangian coordinate, and the map from geostrophic coordinates (X, Z) to physical coordinates $(x, z) = T(X, Z)$ is defined as the map T minimising

$$\int_G \left(\frac{1}{2} \underbrace{(x - X)^2 - Zz(X,Z)}_{=c((x,z),(X,Z))} \right) \sigma \, \mathrm{d}\, X \, \mathrm{d}\, Z,$$

where G is the domain of geostrophic coordinates. Here the minimisation is taken over all maps that transform the density $\sigma \, \mathrm{d}\, X \, \mathrm{d}\, Z$ to the Lesbesgue measure $\mathrm{d}\, x \, \mathrm{d}\, z$. $\sigma \, \mathrm{d}\, X \, \mathrm{d}\, Z$ is obtained as the determinant of the Jacobian of the transformation from physical to geostrophic coordinates, satisfying the continuity equation

$$\sigma_t + \partial_X(U\sigma) + \partial_Z(W\sigma) = 0.$$

To solve these equations, we have to find T, then use it to compute (U, W), and then use (U, W) to transport σ, leading to a new optimal transport problem at the next time instance.

In physical coordinates, the usual fluid dynamical variables can be diagnosed by inverting the transformation since $x - X(x, z)$ is proportional to the out of plane velocity and $Z(x, z)$ is proportional to the temperature.

To progress towards our solver, we first take the Kantorovich relaxation, seeking a joint distribution Π on $G \times \Omega$ (where Ω is the physical domain), that minimises

$$\int_G \int_\Omega c((x, z), (X, Z)) \, \mathrm{d}\, \Pi((x, z), (X, Z)),$$

subject to the constraints that Π has nonnegative measure on any measurable subset of $G \times \Omega$, and Π has marginals given by

$$\int_G \mathrm{d}\, \Pi((x, z), (X, Z)) = \mathrm{d}\, x \, \mathrm{d}\, z, \quad \int_\Omega \mathrm{d}\, \Pi((x, z), (X, Z)) = \sigma \, \mathrm{d}\, X \, \mathrm{d}\, Z.$$

Then, we use the barycentric formula to obtain

$$T(X, Z) = \frac{\int_\Omega (x, z) \, \mathrm{d}\, \Pi((x, z), (X, Z))}{\int_\Omega \mathrm{d}\, \Pi((x, z), (X, Z))}.$$

The entropic regularisation of this problem seeks to minimise the functional,

$$\int_G \int_\Omega c((x, z), (X, Z)) \, \mathrm{d}\, \Pi((x, z), (X, Z)) + \epsilon \int_G \int_\Omega \frac{\delta \Pi}{\delta \nu} \, \mathrm{d}\, \nu,$$

where $\nu = \sigma \, \mathrm{d}\,X \, \mathrm{d}\,Z \times \mathrm{d}\,x \, \mathrm{d}\,z$ is the product measure between template and target. After passing to the Rockafellar dual formulation of this problem (exchanging constraints and cost function), we obtain an optimisation problem for two potentials, ϕ supported on G and ψ on Ω. Iterating the two corresponding optimality conditions defines the Sinkhorn iteration. If we approximate both the template and target measures by sums of Dirac measures, then this Sinkhorn iteration can be easily implemented on a computer.

In my workshop talk I presented numerical results demonstrating the correctness of the method. The method allows a large number of particles to be used (65536 in our example) which goes well beyond previous versions of the geometric algorithm. These numerical results can be found in [1].

REFERENCES

[1] J.-D. Benamou, C.J. Cotter, and H. Malamut, *Entropic optimal transport solutions of the semigeostrophic equations*, Journal of Computational Physics **500** (2024), 112745.
[2] M.J.P. Cullen, *A mathematical theory of large-scale atmosphere/ocean flow*, World Scientific, (2006).
[3] M. Cuturi, *Sinkhorn distances: Lightspeed computation of optimal transport*, Advances in Neural Information Processing Systems **26** (2013).

External forcings, self-organisation and limit cycles of shallow cumulus convection

A. Pier Siebesma

(joint work with Pouriya Alinaghi)

The parameterised representation of shallow cumulus convection remains one of the largest source of uncertainty for cloud representation and cloud feedback strength in general circulation models. The traditional way of parameterising these subgrid clouds is through finding semi-empirical relations between the relevant unresolved cloud parameters such as cloud cover a_c and liquid water path q_c in terms of large scale cloud controlling factors such as the horizontally averaged vertical profiles of temperature, humidity and wind $\{\phi_1, \phi_2 \ldots \phi_n\}$ and the large scale advective tendencies $\{f_1, f_2, \ldots f_n\}$ of these variables

$$(1) \qquad a_c = \mathcal{F}\left(\phi_1, \phi_2 \ldots \phi_n, f_1, f_2, \ldots f_n\right) \qquad q_c = \mathcal{G}\left(\phi_1, \phi_2 \ldots \phi_n, f_1, f_2, \ldots f_n\right)$$

Recent high resolution simulation studies and analyses suggest that shallow cumulus convection is a fundamentally unstable process [1, 2]. Rather than converging to a specific cloudy state (a_c, q_c) for a given mean state as suggested by (1), shallow cumulus clouds tend to aggregate in moist patches that grow larger and become wetter while other dry regions get dryer and also grow in size. During this self-aggregation process also the macroscopic cloud parameters (a_c, q_c) keep developing, in contrast with the traditional parameterization assumption (1).

In order to systematically explore the interplay between the large scale states and the response of the shallow cumulus, roughly 100 Large Eddy Simulations on large domains ($150 \times 150 \, \mathrm{km}^2$) of each 60 hours simulation time have been executed
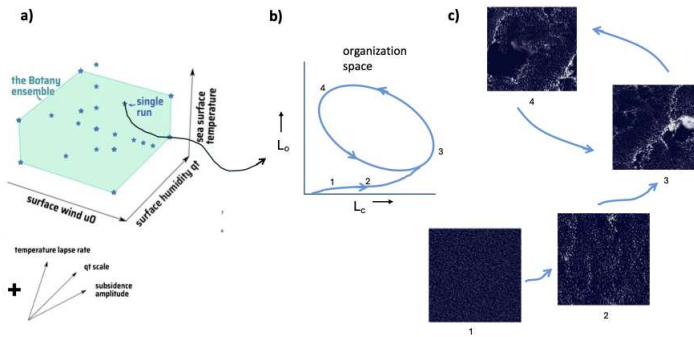
FIGURE 1. Conceptualization of shallow cumulus convection evolution

(Botany dataset) [3]. This simulation ensemble has been carefully selected in order to explore a representative range of all plausible mean states and forcings $\{\phi_1 \ldots \phi_n, f_1, \ldots f_n\}$ that span up an hypercube as illustrated in Fig.1a.

While the simulations produce different cloud fractions and rain rates, most of them develop qualitatively rather similar. Figure 1c shows snapshots of the top view of the cloud albedo for different stages of a typical simulation. During the non-precipitating phase (Figure 1bc, stage 1 and 2), the self-aggregation of the clouds can be observed leading to a growth of the typical horizontal cloud length scale L_c. This aggregation process continues until the cloud clusters have accumulated enough condensed water to initiate precipitation. The resulting rain shafts generate cold downdrafts that counteract the convective updrafts and create cloud free regions (so called cold pools) that temporarily inhibit new cumulus convection. During this phase the cloud system enters into a limit cycle in which periods with large cloud clusters (L_c)and small cloud free areas (L_o) alternate with periods with small cloud clusters and large cloud free areas. This limit cycle is also visible in terms of the cloud macroscopic parameters (a_c, q_c) [4]. In the parlance of mesoscale cloud patterns [5], these findings suggest: Sugar is a transient cloud organization mode while Gravel and Flowers are alternating cloud organization modes that together make up a limit cycle .

Obviously, these preliminary findings invoke many new questions such as

- What is the precise mechanism that cause these limit cycles?
- How do the different external forcings influence the limit cycles in size, frequency and amplitude?
- How effective will the limit cycle behaviour respond to time-varying external forcings (i.e. is the system in quasi-equilibrium)?
- How will radiative effects from the diurnal cycle modify this limit cycle?
- How will the use of more realistic open boundary conditions influence the occurrence of the cloud organisation modes?
- How relevant are these limit cycles for cloud feedback?

REFERENCES

[1] C.S. Bretherton and P.N. Blossey, *Understanding mesoscale aggregation of shallow cumulus convection using large-eddy simulation*, J. of Adv. in Mod. Earth Syst. **9** (2017), 2798–2821.
[2] M. Janssens, J. De Arellano, Jordi Vilà-Guerau, C.C. Van Heerwaarden, S.R. De Roode, A.P. Siebesma and F. Glassmeier, *Nonprecipitating shallow cumulus convection is intrinsically unstable to length scale growth*, Journal of the Atmospheric Sciences **80** (2023), 849–870.
[3] F. Jansson, M. Janssens, J.H. Grönqvist, A.P. Siebesma, F. Glassmeier, J. Attema, V. Azizi, M. Satoh, Y. Sato, H. Schulz and T. Tobias, *Cloud Botany: Shallow Cumulus Clouds in an Ensemble of Idealized Large-Domain Large-Eddy Simulations of the Trades*, Journal of Advances in Modeling Earth Systems **15** (2023), e2023MS003796.
[4] P. Alinaghi, P. Siebesma , F. Jansson, M. Janssens, F. Glassmeier *External Drivers and Self-Organization of Shallow Cold Pools in the Trade-Wind Regime, Subm. to J. of Adv. in Mod. Earth Syst.* (2024), https://essopenarchive.org/users/642912/articles/1182654 .
[5] B. Stevens, S. Bony, Sandrine, H. Brogniez, L. Hentgen, C. Hohenegger, C. Kiemle, T.S. L'Ecuyer, Tristan, A.K. Naumann, H. Schulz, A.P. Siebesma and others *Sugar, gravel, fish and flowers: Mesoscale cloud patterns in the trade winds*, Quarterly Journal of the Royal Meteorological Society **145** (2020), 141–152.

On weak solutions for the inviscid primitive equations

Simon Markfelder

(joint work with Daniel W. Boutros, Edriss S. Titi)

The inviscid primitive equations of oceanic and atmospheric dynamics

$$\nabla_h \cdot u + \partial_z w = 0, \tag{1}$$

$$\partial_t u + u \cdot \nabla_h u + w \partial_z u + \nabla_h p = 0, \tag{2}$$

$$\partial_z p = 0 \tag{3}$$

are an important model in the field of geophysical fluid dynamics [8]. Here u and w denote the two-dimensional horizontal and the scalar vertical velocity respectively, while p is the pressure. All three unknowns u, w, p are functions of time t and the three-dimensional spatial variable $x = (x_1, x_2, z)$. Moreover ∇_h denotes the horizontal gradient, i.e. the gradient with respect to (x_1, x_2). The primitive equations (1)-(3) can be derived as an asymptotic limit of the small aspect ratio (the ratio between vertical and horizontal length scale) from the 3D Euler equations, see e.g. [6].

Onsager conjectured in [7] that weak solutions of the Euler equations which are Hölder continuous in space (uniformly in time) with Hölder exponent $\alpha > \frac{1}{3}$ conserve kinetic energy, while for any $\alpha < \frac{1}{3}$ there exists an α-Hölder continuous weak solution which dissipates energy. Whereas the former was proven already in the 1990's (see [4]), it took until 2018 to prove the second part (see [5, 3] and references therein). The technique which solved the latter is called *convex integration*, which allowed to construct examples of weak solutions with the desired properties.

Our goal is to formulate and prove an Onsager statement for the inviscid primitive equations (1)-(3).

In order to take their anisotropic structure into account, we introduce a new notion of weak solutions for the inviscid primitive equations (1)-(3) in [1]. Roughly speaking, the vertical velocity w of this new type of weak solutions is only required to be a distribution. In [1] we state an analogue of Onsager's conjecture in the context of the inviscid primitive equations for both the classical (where all components of the velocity are understood as functions) and the new notion (where the vertical velocity w is treated as a distribution, see above) of weak solution. Also in [1] we prove the conservation parts of the aforementioned conjectures, i.e. we show that energy is conserved if the solution is sufficiently regular.

In [2] we develop a convex integration scheme to prove the existence and nonuniqueness for the new type of weak solutions (more precisely, for a further generalization of those), and also to exhibit examples of this kind of weak solutions which do not conserve energy. This can be viewed as the first step towards proving the dissipation parts of the Onsager-type conjectures from [1].

Surprisingly, our convex integration approach can be also applied to the *two-dimensional* inviscid primitive equations, as well as the three-dimensional *viscous* primitive equations, and the two-dimensional Prandtl equations.

References

[1] D. Boutros, S. Markfelder and E. Titi, *On Energy Conservation for the Hydrostatic Euler Equations: An Onsager Conjecture*, Calc. Var. Partial Differential Equations **62** (2023), Article No. 219.

[2] D. Boutros, S. Markfelder and E. Titi, *Nonuniqueness of Generalised Weak Solutions to the Primitive and Prandtl Equations*, J. Nonlinear Sci. **34** (2024), Article No. 68.

[3] T. Buckmaster, C. De Lellis, L. Székelyhidi Jr. and V. Vicol, *Onsager's conjecture for admissible weak solutions*, Comm. Pure Appl. Math. **72** (2018), 229–274.

[4] P. Constantin, W. E and E. Titi, *Onsager's conjecture on the energy conservation for solutions of Euler's equation*, Comm. Math. Phys. **165** (1994), 207–209.

[5] P. Isett, *A proof of Onsager's conjecture*, Ann. of Math. (2) **188** (2018), 871–963.

[6] J. Li and E. Titi, *The primitive equations as the small aspect ratio limit of the Navier-Stokes equations: Rigorous justification of the hydrostatic approximation*, Journal de Mathématiques Pures et Appliquées **124** (2019), 30–58.

[7] L. Onsager, *Statistical hydrodynamics*, Nuovo Cimento (9) **6** (1949), 279–287.

[8] L. Richardson, *Weather Prediction by Numerical Process*, Cambridge University Press (1922).

An introduction to rough paths
Martin Hairer

The theory of rough paths [1, 2] provides a *deterministic* theory of integration that is flexible enough to cover the kind of stochastic integrals arising in the theory of (smooth) stochastic differential equations, even with driving noises that are rougher than Brownian motion. The main idea is to view the integrator W as a *rough path* $\mathbf{W}$ which, in the case of regularity $\alpha \in (1/3, 1/2)$, consists of a *pair* $\mathbf{W} = (W, \mathbb{W})$ where $W \in C^\alpha(\mathbb{R}, \mathbb{R}^n)$ is the "usual" integrator, while $\mathbb{W} \colon \mathbb{R}^2 \to$

$\mathbb{R}^n \otimes \mathbb{R}^n$ is an "enhancement" satisfying the Hölder-type analytic bound $\|\mathbb{W}_{s,t}\| \lesssim |t-s|^{2\alpha}$, as well as the algebraic constraint

$$\mathbb{W}_{s,t} - \mathbb{W}_{s,u} - \mathbb{W}_{u,t} = W_{s,u} \otimes W_{u,t} \,, \tag{1}$$

where $W_{s,t} = W_t - W_s$. The idea is that one should think of $\mathbb{W}_{s,t}$ as specifying values for the integrals $\int_s^t W_{s,u} \otimes dW_u$, with the above constraint encoding the facts that "constants can be pulled out of integrals" and "integrals are additive under concatenation of integration domains".

A natural class of integrands is then provided by functions that "locally look like W", also called "controlled rough paths". More precisely, a control rough path consists of a pair (Y, Y') of α-Hölder continuous functions such that furthermore the remainder $R_{s,t} = Y_{s,t} - Y_s' W_{s,t}$ satisfies the bound $\|R_{s,t}\| \lesssim |t-s|^{2\alpha}$.

One then defines the integral of Y against W by the limit of compensated Riemann sums

$$\int_u^v Y_r dW_r = \lim_{|\mathcal{P}| \to 0} \sum_{[s,t] \in \mathcal{P}} \left(Y_s W_{s,t} + Y_s' \mathbb{W}_{s,t} \right) \,, \tag{2}$$

where $\mathcal{P}$ denotes a partition of $[u,v]$ into disjoint intervals. In this talk, we showed how that notion of integral can be used to define solutions to "rough" differential equations of the type

$$dY = F(Y)dW \,, \tag{3}$$

and how it can be used to analyse two-scale problems.

REFERENCES

[1] T. Lyons, *Differential equations driven by rough signals*, Revista Matemática Iberoamericana **14**, vol. 2 (1998), 215–310.
[2] M. Hairer, P. Friz, *A course on rough paths*, Universitext, Springer (2020), xvi+346 pp.

Evaluating a multiscale asmptotic approximation for synoptic and mesoscale motions in the midlatitude atmosphere

GEORGE CRAIG

(joint work with Tobias Selz, Mirjam Hirt)

Weather in the midlatitudes is dominated by phenomena on two scales. The first is synoptic cyclones, on scales of order 1000 km, driven by the pole to equator temperature gradient, and approximately following geostrophic balance. The second is convective storms, on scales up to order 100 km, driven by conditional instability in the vertical direction (where the stratification is rendered unstable by condensation and release of latent heat in ascending air), and dominated by divergent flows. In a comprehensive review of approximate equations for different atmospheric regimes, [4] identified suitable single-scale asymptotic approximations for advection-dominated motions on the midlatitude synoptic and meso-scales. These are the quasi-geostrophic equations (QG) for nearly geostrophic motions on the

synoptic scale, and the hydrostatic weak temperature gradient equations (WTG) for motions with strong diabatic heating on the mesoscale.

In an earlier study, we used output of a high resolution weather prediction model to compute a number of different dimensionless parameters as function of length and time scale [2]. These included the Rossby number, which should be small for quasi-geostrophic theory to apply, and a version of the Froude number, which should be small for flows close to weak temperature gradient balance. These parameters were indeed found to be relatively small on the respective scales identified by [4], confirming that the proposed leading order dynamics should be relevant for motions on these scale. It should be noted however, that while the parameters were small, they were not very small ($Ro \sim 0.2$, $Fr^2 \sim 0.5$), indicating that while the QG and especially the WTG approximations might be useful to gain insight, they would not produce quantitatively accurate solutions.

Based on these early results, we then employed the method of multi-scale asymptotic analysis to derive a two-scale asymptotic approximation to the equations of motion, that would reproduce the leading order dynamics of the single-scale approximations and also introduce consistent scale interaction terms linking the two regimes [3]. The motivation for this was threefold. First, we were interested in large-scale control of thunderstorm movement, the basis of nowcasting. Second, we hoped for insight into the upscale influence, or often lack of influence, of small-scale perturbations introduced by stochastic parameterization schemes that model variability due to unresolved motions in weather prediction models. Finally we wished to examine the processes of upscale error growth, causing the butterfly effect.

In Oberwolfach, some new results were presented, where we evaluated the accuracy of the approximate mesoscale and synoptic equations using output of the global ICON numerical weather prediction model, with a horizontal resolution of about 10 km, 120 vertical levels, and an analysis region confined to a midlatitude band. The first task was to separate the atmospheric variables into different space and time scale bands. Doing this, we immediately identified an incorrect assumption in the formulation of [3], where it was assumed that the magnitudes of the synoptic and mesoscale horizontal winds were comparable, when in fact the mesoscale wind was at least an order of magnitude weaker. Fortunately, this assumption is easy to change by setting the first term in the mesoscale horizontal wind expansion to zero in the Appendix of [3] and following the subsequent steps of the derivation. The resulting mesoscale equations are WTG balance for vertical motion:

$$w_2 \partial_z \overline{\theta} = Q_{\theta,3},$$

continuity:

$$\nabla_m \cdot \vec{v}_{1,m} + \frac{1}{\bar{p}} \partial_z \left(\bar{p} w_2 \right) = 0.$$

and the equation for the vertical component of mesoscale vorticity:

$$\partial_{t_m} \zeta_m + \vec{v}_{0,s} \cdot \nabla_m \zeta_m + f_0 \nabla_m \cdot \vec{v}_{1,m} + \vec{k} \cdot \left(\nabla_m w_2 \times \partial_z \vec{v}_{0,s} \right) = \vec{k} \cdot \nabla_m \times Q_{\vec{v},1}.$$

The synoptic equations express geostrophic and hydrostatic balance:

$$\vec{k} \times \vec{v}_{0,s} = \nabla_s \pi_0, \ \partial_z \pi_0 = \theta_0,$$

continuity of the ageostrophic wind:

$$\nabla_s \cdot \vec{v}_{1,s} + \frac{1}{\bar{p}} \partial_z \left(\bar{p} w_{3,s} \right) = 0,$$

and the evolution of the QG potential vorticity

$$\partial_{t_s} q_s + \nabla_s \cdot (\vec{v}_{0,s} q_s) = \frac{f_0}{\bar{p}} \partial_z \left(\frac{\bar{p}}{\partial_z \bar{\theta}} \overline{Q_{\theta_4}} \right).$$

As these equations show, the main downscale influence of the synoptic scale is an advection that transports mesoscale vorticity features with the synoptic wind. Surprisingly, there is no upscale influence of the mesoscale at leading order. The weak temperature gradient approximation smooths the small scale thermal anomalies, while the mesoscale wind is too weak to impact the stronger synoptic vorticity field.

The quantitative evaluation of the terms in these equations confirmed that for both scales of motion the equations were approximately satisfied, with one notable exception. The magnitude of the residual in the mesoscale vorticity equation was about 40% of the size of the retained terms, which is consistent with the expected squared Froude number of about 0.5. On the other hand, the residual in the synoptic QGPV equation was comparable in size to the other terms, and almost exactly the negative of the diabatic heating term. This is not consistent with the approximation and points to an incorrect assumption in the scaling. An interesting possibility that emerged at the workshop is that rather than targeting QG dynamics at leading order, it might be more appropriate to choose the semigeostrophic approximation. This would introduce an adiabatic cooling term in the PV equation that would compensate the diabatic heating. However, the derivation of the semigeostrophic approximation involves an unconventional scaling assumption [1], and may be difficult to incorporate consistently in the multiscale analysis.

So what have we learned about the problems that motivated the study? First, the synoptic advection of mesoscale features has been correctly identified as the most important downscale influence. Second, the absence of upscale influences due to the smoothing of mesoscale temperture perturbations by WTG dynamics provides a theoretical explanation of why stochastic parameterizations in operational weather prediction systems must perturb the model on synoptic scales to have an effect there, despite the strong impact of small-scale perturbations on the mesoscale variability. The upscale growth of small initial errors has not yet been addressed in this work.

References

[1] Craig, George C., *A Scaling for the Three-Dimensional Semigeostrophic Approximation.* Journal of the Atmospheric Sciences **50** (1993): 3350–55.

[2] Craig, George and Tobias Selz *Mesoscale Dynamical Regimes in the Midlatitudes.* Geophysical Research Letters **45** (2018): 410-417.

[3] Hirt, Mirjam, George C. Craig, and Rupert Klein. *Scale Interactions between the Meso- and Synoptic Scales and the Impact of Diabatic Heating.* Quarterly Journal of the Royal Meteorological Society **149**, (2023): 1319–34.

[4] Klein, Rupert. *Scale-Dependent Models for Atmospheric Flows.* Annual Review of Fluid Mechanics **42**, (2010): 249–274.

From Blocks to Nambu mechanics

ANNETTE RUDOLPH

(joint work with Lisa Schielicke, Péter Nevir)

Atmospheric blocks are long-lasting weather patterns that block the westerly flow for several days to months. These large-scale weather patterns can cause extreme precipitation and draughts. The persistence of blocks can be explained by the so-called point vortex theory. This discrete vortex theory for 2D adiabatic and inviscid flows was introduced by [2] and [4]. [6] and [3] show that this concept can be transferred to so-called omega blocks, where an anticyclone in the north is accompanied by two cyclones southwest and southeast of the anticyclone. If they lie on an equilateral triangle and if the sum of the circulations of the three vortices is zero, the three vortices form a so-called relative equilibrium. The authors show that the translational velocity of this vortex configuration is in the same order of magnitude as the basic flow, which explains the stationarity of the omega block. This concept, together with the kinematic vorticity number [11], leads to an algorithm, that identifies an atmospheric block as well as each individual vortex of the block. Based on this algorithm, [1] analyze the occurrence of the different blocks (high-over-low and omega blocks) and show shifts in the seasons of the occurrence of blocks, which can have huge impacts on e.g. vegetation.

Point vortex motion can also be viewed from the Nambu perspective. [8] introduced a generalization of canonical Hamiltonian mechanics of discrete systems. He generalized the bilinear, antisymmetric Poisson bracket to a trilinear, twice antisymmetric bracket – now called the Nambu bracket. Regarding Nambu's formulation, the dynamics of a system with N degrees of freedom is described by $N-1$ conserved quantities. This is in contrast to Hamilton's formulation, which only considers the energy. Therefore, more physical information can be captured using Nambu's formalism. Regarding point vortex dynamics, two conserved quantities, the energy H and the relative angular momentum M, can be used to formulate the equation of motion in the three-dimensional phase space of the relative distances $r_i,\ i = 1, 2, 3$, $\mathbf{r} = (r_1, r_2, r_3)$ between three point vortices:

$$\rho \frac{d\mathbf{r}}{dt'} = \nabla M \times \nabla H$$

where the time t is scaled by a constant factor $\alpha \in \mathbb{R}$, $t' = \alpha$, $\alpha = \sigma/2\Gamma_1, \Gamma_2, \Gamma_3$, where Γ_i denotes the circulation of the i-th vortex, $\sigma \in \mathbb{R}$. In this way, the trajectory of three point vortices is given by the intersection line(s) of the two surfaces that are given by the two conserved quantities [5].
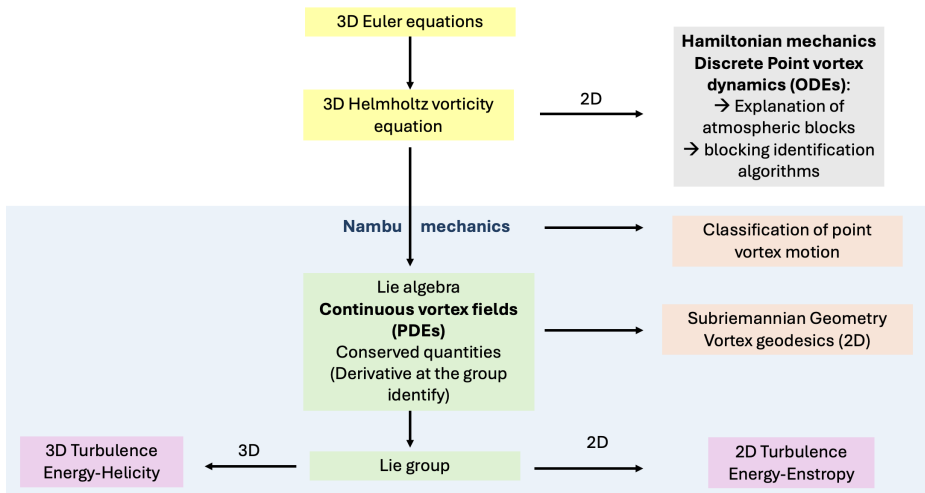
FIGURE 1. Nambu mechanics allows for a derivation of a Lie al-
gebra and Lie group based on multiple conserved quantities.

[9] transferred Nambu's idea to continuous vortex flows in two and three spatial
dimensions. According to their representation of vortex flows, the kinetic energy
and a vortex-related quantity play an equal role in the representation of the vortex
motion. The choice of the vortex-related quantity depends on the spatial dimension
(2D: enstrophy, 3D: helicity). Let $\boldsymbol{\xi}$ be the 3D vorticity vector, h the helicity and
$\mathcal{H}$ the energy. For an arbitrary functional $\mathcal{F}$ that depends on the vorticity vector,
the time evolution under adiabatic, invsicid conditions is given by:

$$(1) \qquad \{\boldsymbol{F}, h, \mathcal{H}\} = -\int_V d\tau \left(\left(\nabla \times \frac{\delta\mathcal{F}}{\delta\boldsymbol{\xi}} \right) \cdot \left(\nabla \times \frac{\delta h}{\delta\boldsymbol{\xi}} \right) \times \left(\nabla \times \frac{\delta\mathcal{H}}{\delta\boldsymbol{\xi}} \right) \right).$$

The time evolution of the vorticity results from $\mathcal{F} = \boldsymbol{\xi}$. Moreover, the Nambu
bracket of the components of the momentum, the total flux of vorticity w.r.t the
helicity generate a Lie algebra [10] from which a Lie group for vortex flows can be
derived [7]. First applications of this group theoretical approach to splitting storms
suggest that this Lie group may be of interest for further research in the field of
turbulence. One example is that the 3D Nambu bracket that generate the Lie
algebra/Lie group is determined in terms of helicity (not in terms of the energy,
which can be added by another bracket). Therefore helicity can be considered
separately from the energy. Furthermore, the Nambu brackets are derived under
the assumption of conservative systems. Therefore, one hypothesis, which may be
a topic for further research, is that friction is only related to the direction of the
cascade and not to the mechanism of vortex splits. Fig. 1 provides an overview of
the topics and interrelationships addressed in the presentation.

References

[1] C. Detring, A. Müller, L. Schielicke, P. Névir, and H. W. Rust. *Occurrence and transition probabilities of omega and high-over-low blocking in the Euro-Atlantic region*, Weather and Climate Dynamics, **2**, (2021) 927–952,

[2] H. Helmholtz, *Über hydrodynamischer Gleichungen welche den Wirbelbewegungen entsprechen.* J. Reine Angew. Math, **5** (1858) 25–55.

[3] M. Hirt, L. Schielicke, A. Müller, and P. Névir, *Statistics and dynamics of blockings with a point vortex model.* Tellus A, **70**(1) (2018) 1458565.

[4] G. Kirchhoff, Vorlesungen über mathematische Physik I, volume 1, 1876 Teubner.

[5] A. Müller, and P. Névir, *A geometric application of Nambu mechanics: the motion of three point vortices in the plane.* Journal of Physics A: Mathematical and Theoretical, **47**(10) (2014) 105201

[6] A. Müller, and P. Névir, L. Schielicke, M Hirt, J Pueltz, and I. Sonntag, *Applications of point vortex equilibria: blocking events and the stability of the polar vortex.* TellusA, **67** (2015).

[7] A. Müller, and P. Névir, *On the algebra and groups of incompressible vortex dynamics*, J. Phys. A: Math. Theor., **54** (30) (2021) 305203

[8] Y. Nambu, *Generalized Hamiltonian dynamics.* Physical Review D, **7**(8) (1973) 2405.

[9] P. Névir and R. Blender. *A Nambu representation of incompressible hydrodynamics using helicity and enstrophy.* Journal of Physics A: Mathematical and General, **26**(22) (1993) L1189.

[10] P. Névir. *Die Nambu-Felddarstellungen der Hydro-Thermodynamik und ihre Bedeutung für die dynamische Meteorologie.* Habilitation dissertation, Freie Universität Berlin, 1998

[11] L. Schielicke, P. Névir, U. Ulbrich. *Kinematic vorticity number- a tool for estimating vortex sizes and circulations.* Tellus A, **68** (2016)

Rigorous analysis and numerical implementation of nudging data assimilation algorithms

Edriss Titi

We introduce downscaling data assimilation algorithms for weather and climate prediction on discrete coarse spatial scale measurements of the state variables (or only part of them, depending on the underlying model). The algorithms are based on linear nudging of the algorithms' solution towards the coarse spatial scales corresponding to the observed measurements of the unknown reference solution. The algorithms are initialized arbitrarily and are known to converge at exponential rate toward the exact unknown reference solution. This indicates that the dynamics of the algorithms are globally stable (not chaotic), unlike the dynamics of the model that governs the unknown reference solution. Capitalizing on this fact, we also show uniform in time error estimates of numerical discretizations of these algorithms, which makes them reliable upon implementation computationally. Furthermore, we present recent improvement of those algorithms by employing nonlinear nudging, which yields super-exponential convergence rate toward the unknown reference solution.

Atmospheric flow regimes: stochastic modelling and data clustering for sensitivity studies and reduced stochastic models

Nikki Vercauteren
(joint work with Vyacheslav Boyko, Amandine Kaiser, Sebastian Krumscheid)

Multistability is a frequent feature in the climate system and leads to key challenges for our ability to predict how the system will respond to transient perturbations of the dynamics. As a particular example, the stably stratified atmospheric boundary layer is known to exhibit distinct flow regimes that are believed to be metastable. Numerical weather prediction and climate models encounter challenges in accurately representing these flow regimes and the transitions between them, leading to an inadequate depiction of regime occupation statistics. We use a hierarchy of models to improve theoretical understanding of the system, specifically focusing on the mechanisms that could lead to metastability and on the sensitivity of the system to transient perturbations in the dynamics. The simplest models presented were stochastic conceptual models, used as a tool to systematically investigate what types of unsteady flow features may trigger abrupt transitions in the mean boundary layer state. The numerical findings show that simulating intermittent turbulent mixing may be key in some cases, where transitions in the mean state follow from initial transient bursts of mixing.

Turbulent mixing is a parameterized process in atmospheric models, and the theory underpinning the parameterization schemes was developed for homogeneous and flat terrain, with stationary conditions. The parameterized turbulent mixing lacks key spatio-temporal variability that induces transient perturbations of the mean dynamics. This variability could be effectively included via stochastic parameterisation schemes, provided one knows how to define the strength or memory characteristics of random perturbations. Towards that goal, we use a systematic data-driven approach to quantify the uncertainty of parameterisations and inform us on how and when to incorporate uncertainty using stochastic models. To enable such a systematic data-driven approach, methods from entropy-based learning and uncertainty quantification were combined in a model-based clustering framework, where the model is a stochastic differential equation with piecewise constant parameters [1]. As a result, stochastic parameterisation can be learned from observations. The method is able to retrieve a hidden functional relationship between the parameters of a stochastic model and the resolved variables. A reduced model is obtained, where the unresolved scales are expressed as stochastic differential equations whose parameters are continuous functions of the resolved variables. Using field measurements of turbulence, the stochastic modelling framework is able to uncover a stochastic parameterisation that represent unsteady mixing in difficult conditions [2]. Such methodology will be explored for further derivation of stochastic parameterisations, and should help to quantify uncertainties in climate projections related to uncertainties of the unresolved scales dynamics.

<div align="center">REFERENCES</div>

[1] V. Boyko, S. Krumscheid, N. Vercauteren *Statistical Learning of Nonlinear Stochastic Differential Equations from Nonstationary Time Series using Variational Clustering*, Multiscale Modeling & Simulation **20,4** (2022), 1251–1283.

[2] V. Boyko, N. Vercauteren *A stochastic stability equation for unsteady turbulence in the stable boundary layer*, Quarterly Journal of the Royal Meteorological Society **149, 755** (2023), 2125–2145.

Identification of Atmospheric Blocking patterns: High-over-Low and Omega Blocks

<div align="center">LISA SCHIELICKE</div>

Blocking is a synoptic-scale, quasi-stationary atmospheric phenomenon in the mid-latitudes, significantly influencing regional weather for days to weeks. Typically, a blocking pattern consists of a high-pressure system poleward of one or two low-pressure systems, obstructing the typical westerly flow. A two-vortex configuration is known as a high-over-low or Rex block, while a three-vortex configuration is called an Omega block, resembling the Greek letter Omega. Blocks are associated with high-impact weather such as heatwaves and extreme precipitation events due to their quasi-stationary nature.

Although many methods exist to identify blocked periods, a reliable method to differentiate between high-over-low and Omega blocks has not been made publicly available so far. In this work, I present a method that is able to differentiate between these blocking patterns, assuming the associated vortices are synoptic in scale (horizontal length scale of 1000 km) and behave like a point vortex ensemble. The method provides information on block properties such as time, location, vortex circulation, size, and blocking type. Additionally, it can pinpoint regions of high-impact weather associated with blocks.

The process to identify the type of blocking has two steps. The first step is based on a kinematic vortex identification technique (kinematic vorticity number W_k method) that reliably extracts vortex properties from the three-dimensional flow field, as demonstrated in previous studies [1, 4, e.g.]. The kinematic vorticity number W_k is defined as the ratio of the local rotation rate $\|\Omega\|$ and strain rate $\|S\|$ as

$$(1) \qquad W_k = \frac{\|\mathbf{\Omega}\|}{\|\mathbf{S}\|} \text{ with } \mathbf{\Omega} = \frac{1}{2}\left(\nabla\mathbf{v} - (\nabla\mathbf{v})^T\right) \ . \mathbf{S} = \frac{1}{2}\left(\nabla\mathbf{v} + (\nabla\mathbf{v})^T\right)$$

Here, $\mathbf{\Omega}$ and $\mathbf{S}$ are the antisymmetric and symmetric parts of the velocity gradient tensor, respectively. A vortex is defined as a simply-connected region where $W_k > 1$, indicating that rotation prevails over strain rate within the vortex. To identify atmospheric vortices, the W_k number is calculated at each grid point of the flow field. Subsequently, a vortex field is generated by setting each grid point below a threshold (generally $W_k \leq 1$) to zero and all other points to one. When applied to two-dimensional data, the sense of rotation (cyclonic or anticyclonic)

is used to distinguish between lows and highs. Additionally, the method allows to determine vortex sizes, intensities (circulations) and their locations (circulation centers).

Furthermore, to identify the blocking pattern, the method utilizes concepts from point vortex theory. A point vortex is a vortex of zero size, located at a specific point in the two-dimensional flow field. While its vorticity is infinitely high, the vortex's circulation remains constant. Each point vortex induces a circular velocity field proportional to the vortex's circulation and decreases inversely with the distance from the vortex. The motion of a point vortex is determined by the velocities induced by all other point vortices in the field. Additionally, a point vortex ensemble moves around its center of circulation. Under certain conditions – such as zero total circulation and specific configurations (a high on the poleward side of the low in a high-over-low block or an equilateral triangle with two lows in an Omega block) – a point vortex ensemble of two or three vortices will move westward, countering the typical westerly flow of the midlatitudes.

In the second step of the identification method for high-over-low or Omega blocking, we search for the blocking pattern that minimizes total circulation and satisfies the vortex configuration according to point vortex theory. Starting with a box that surrounds the high, we extend the box southward and search for the minimum total circulation within this expanded box. Simultaneously, we search for the minimum total circulation in a trapezoidal shape whose lower border is also extended southward, while the sides are allowed to grow east- and westward. Finally, we inspect the circulation directly south of the high and east- and westward south of the high to determine if the block is a high-over-low or an Omega block.

In previous work, we have observed that the method provides reasonable values for vortex properties and blocking motion speeds [3, 2]. Additionally, we have investigated the transition probabilities between blocking and non-blocking states in the Euro-Atlantic sector, along with their seasonal behavior and changes over the 30-year period from 1990 to 2019 [5].

Currently, the identification method is tested on daily reanalysis (ERA5) and seasonal forecast data, focusing on high-precipitation events in Europe. This work is in collaboration with Annette Rudolph (TU Berlin, Germany) and Gregor Leckebusch (University of Birmingham, UK) and his team. The Python code for the method will soon be made available.

REFERENCES

[1] L. Schielicke, P. Névir, U. Ulbrich *Kinematic vorticity number–a tool for estimating vortex sizes and circulations*, Tellus A: Dynamic Meteorology and Oceanography **68,1** (2016), 29464.

[2] M. Hirt, L. Schielicke, A. Müller, P. Névir *Statistics and dynamics of blockings with a point vortex model*, Tellus A: Dynamic Meteorology and Oceanography **70,1** (2018), 1–20.

[3] A. Müller, P. Névir, L. Schielicke, M. Hirt, J. Pueltz, I. Sonntag *Applications of point vortex equilibria: blocking events and the stability of the polar vortex*, Tellus A: Dynamic Meteorology and Oceanography **67,1** (2015), 29184.

[4] L. Schielicke, C.P. Gatzen, P. Ludwig *Vortex identification across different scales*, Atmosphere **10,9** (2019), 518.

[5] C. Detring, A. Müller, L. Schielicke, P. Névir, H.W. Rust *Occurrence and transition probabilities of omega and high-over-low blocking in the Euro-Atlantic region*, Weather and Climate Dynamics **2,4** (2021), 927–952.

Statistical and dynamical models for Indian summer monsoon

Amit Apte

The Indian summer monsoon is a multiscale, multiphysics phenomena that exhibits significant variability both in short (seasonal) and long (year-to-year) time scales, as well as over multiple spatial scales [5, 1]. An understanding of the basic dynamical system of the monsoon, including the role of the seasonal migration of the inter-tropical convergence zone and the land-ocean temperature contrast, is an important open problem in climate sciences [4]. We study two different types of models that capture different aspects of this complex phenomena, though admittedly do not directly address the issues mentioned above. The long-term goal is to formulate methodologies for relating and drawing inferences from such disparate models in order to better understand and predict tropical processes in general and the monsoon in particular, at multiple scales from seasonal to decadal variability.

We propose [2, 3] a representation of the Indian summer monsoon rainfall in terms of a probabilistic model based on a Markov random field consisting of discrete state variables representing low and high rainfall at grid-scale and daily rainfall patterns across space and in time. These discrete states are conditioned on observed daily gridded rainfall data from the period 2000 to 2007.

Using Gibbs sampling of the posterior distribution for the discrete random variables conditioned on the observed rainfall, we identify clusters (of the days and locations) and then obtain the prominent rainfall patterns (spatial and temporal, respectively). The spatial patterns are shown in figure 1.
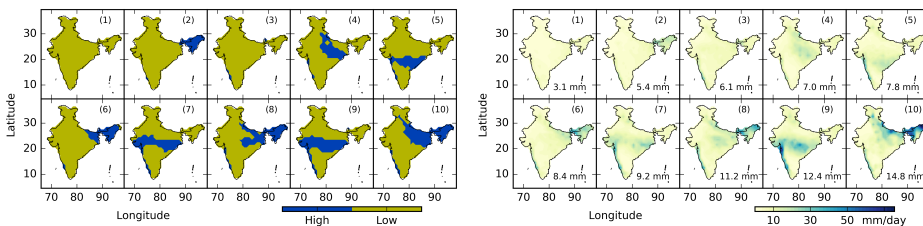
FIGURE 1. Prominent canonical discrete patterns (CDP), and the corresponding canonical rainfall patterns (CRP) identified by the MRF model.

We also study a Markov chain model based on the transition between these patterns and find relations to the active-break phases of the monsoon as well as regional wet and dry spells during the monsoon season. The application of this general methodology to other spatio-temporally varying processes is a problem of general interest for future investigations.

REFERENCES

[1] Sulochana Gadgil. The indian monsoon and its variability. *Annual Review of Earth and Planetary Sciences*, 31:429–467, 2003.
[2] Adway Mitra, Amit Apte, Rama Govindarajan, Vishal Vasan, and Sreekar Vadlamani. A discrete view of the Iindian monsoon to identify spatial patterns of rainfall. *Dynamics and Statistics of the Climate System*, 3(1):dzy009, 2018.
[3] Adway Mitra, Amit Apte, Rama Govindarajan, Vishal Vasan, and Sreekar Vadlamani. Spatio-temporal patterns of daily Indian summer monsoon rainfall. *Dynamics and Statistics of the Climate System*, 3(1):dzy010, 2018.
[4] D R Sikka and Sulochana Gadgil. On the maximum cloud zone and the itcz over indian, longitudes during the southwest monsoon. *Monthly Weather Review*, 108(11):1840–1853, 1980.
[5] Peter J Webster, Vo Oo Magana, TN Palmer, J Shukla, RA Tomas, MU Yanai, and T Yasunari. Monsoons: Processes, predictability, and the prospects for prediction. *Journal of Geophysical Research: Oceans*, 103(C7):14451–14510, 1998.

Atmospheric dynamics of giant planets

YOHAI KASPI

The giant planets of the Solar System, Jupiter, Saturn, Uranus and Neptune exhibit some of the most striking dynamical phenomena in the Solar System, such as multiple jet-streams, long-lived cyclones and turbulent convection. In this talk, we will review the physical mechanisms governing the dynamics on these planets. Particular focus will be given to recent new measurements from NASA's Juno and Cassini spacecraft, which have been orbiting Jupiter and Saturn, respectively, in recent years.

On Jupiter the jet streams dominate the midlatitudes between 15° and 65° latitude in both hemispheres. Poleward of these latitudes, the atmosphere is more turbulent containing mainly floating cyclones and anticyclones, while equatorward a broad eastward flow dominates the equatorial region. Over the past 8 years, with now over 60 polar orbits of Jupiter, the Juno mission has revolutionized the way we understand the Jovian atmosphere. It revealed details about these three distinct regions, revealing very different dynamics in each of them. Here we will review the dynamics of each of them.

The polar region: Juno's IR mapper (JIRAM) revealed that the poles are dominated by a system of cyclones surrounding a central polar cyclone with five circumpolar cyclones around the south pole and eight such cyclones around the north pole. The cyclones are held together by vorticity dynamics balancing the overall tendency of cyclones to drift poleward (beta-drift). In addition, the cyclones have been observed to drift westward and oscillate over the duration of the mission, which can be also explained by these dynamical considerations. We will review the mechanisms driving the dynamics of these cyclones and discuss their stability and long-term temporal behavior.

The midlatitudes: Juno's gravity measurements, which remarkably have been able to provide gravity harmonics up to J40, have revealed the overall depth of the midlatitude jet-streams being 3000 km, and have confirmed previous theories
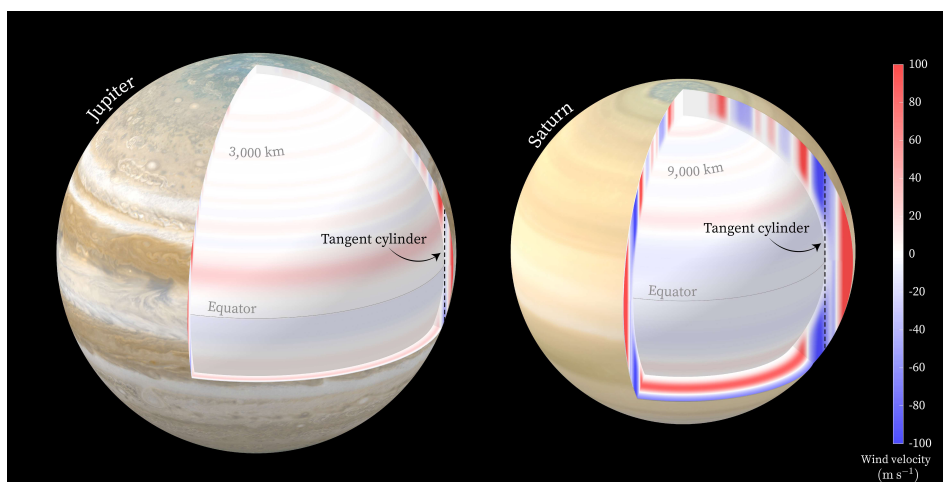
FIGURE 1.

showing that the flows penetrate inward in a direction parallel to the spin axis. This depth, deduced by the gravity measurements is consistent with the depth where electrical conductivity rises due to the gas becoming denser with depth, and thus hints to the role of the magnetic field in halting the flows at depth. We will also show Cassini gravity measurements for Saturn revealing the Saturnian jets streams are three times deeper, consistent with the mass of Saturn being only a third of that of Jupiter and thus becomes of comparable density deeper. Juno's microwave measurements revealed that the midlatitude jets are accompanied by a series of meridional circulation cells (similar to Earth's Ferrel cells), which accompany each one of the midlatitude jet-streams. The jets are held together by upgradient Reynold stresses which drive these east and west flows and the same fluxes also drive the meridional circulation. We will show the governing equations and the consistency with the observations.

The equatorial region: Both Jupiter and Saturn have very strong zonal prograde flows near the equator. The equatorial region on Jupiter reaches latitude 17° while on Saturn it reaches about 32° in both hemispheres. These values are also consistent with the depth of the flows on both planets taking into account the cylindrical projection of the 3000 and 9000 km depth of the flows on both planets. The equatorial flows are also super-rotating, meaning that there must be an angular momentum source in this region. We show how such flows can develop and how the Reynolds stresses perpendicular to the rotation axis and converging towards the equator can drive these flows as well. Thus, the gravity measurements also provided an explanation to the nature of the superrotating equatorial flow and how it compares to that of Saturn. Microwave and gravity measurements also allowed putting constraints on Jupiter's Great Red Spot, showing that it penetrates between 300 and 500 km deep. In this talk, we will give an overview of these

discoveries by Juno and provide an overview of the governing dynamics in each of these regimes.

A hierarchy of models to understand the deep ocean structure and circulation

Raffaele Ferrari

(joint work with Mason Rogers, Louis-Philippe Nadeau)

Recent theoretical work suggests that abyssal waters rise toward the surface primarily along the sloping boundaries of ocean ridges and seamounts. These topographic features are characterized by vigorous turbulent mixing along the seafloor generated by tidal flows sloshing waters over the corrugated topography [1, 2]. The goal of this presentation is to investigate the physics of the upslope flows and discuss their relevance for the global ocean circulation.

We started by presenting new results from a recent observational campaign conducted along the corrugated topography of the Rockall Trough, a 2000-deep trough west of Ireland. The observational team injected a fluorescent dye at the bottom of a canyon cutting through the eastern boundary of the trough. The dye was then sampled over the next two days with fluorometers providing uncontrovertible evidence of a strong flow up the canyon slope at a rate of 100 m per day, the largest upslope flow ever recorded in the abyssal ocean [3]. Concurrent measurements from turbulent probes mounted along bottom-anchored moorings showed that every tidal period a 200 m tall patch of turbulence developed along the seafloor [4].

We proceeded to describe the physics that generates the observed turbulent events. The turbulence appears to be triggered by an instability of the tidal flow sloshing back and forth along the sloping canyon. The reversing tidal flow is generated by the semidiurnal tidal potential and varies linearly in the vertical between 0 and 20 cm/s over the 300 m depth of the canyon. The canyon water is stably stratified, meaning that the water density decreases away from the seafloor. It is well known that a steady horizontal sheared flow in a stratified fluid is unstable to the Kelvin-Helmholtz instability [5, 6] if the shear is sufficiently strong. The observed tidal shear is too weak to undergo the classical Kelvin-Helmholtz instability. We therefore explored the impact of a sloping boundary and a time-varying sheared flow. The slope has a minor effect on the instability while the time dependence does. Using Floquest theory we demonstrated that the sheared tidal flow is unstable and that this instability triggers the turbulence events.

Next, we discussed how the turbulence drives an upslope flow. The turbulent events mix the stratified water on a vertical scale of about 200 m. The turbulence therefore mixes overlying lighter water with denser one along the seafloor. As the bottom water gets lighter through mixing, it starts rising along the sloping seafloor resulting in a net upslope flow. Scaling arguments and numerical simulations confirmed that the mixing generated by the turbulence is sufficient to explain the strength of the upslope flow.

Last, we showed how the mixing along sloping topography and the resulting upslope flows connect to the ocean abyssal circulation and density distribution. Ocean waters sink into the abyss at high latitudes in response to strong air-sea cooling and brine rejection, when waters freeze [7]. Modern estimates suggest that about $30 \times 10^6 \, \mathrm{m}^3$ of water sinks into the abyss every second or about the equivalent of the transport by 15 Amazon Rivers. The upslope flow along seamounts and ridges represents the return branch of the abyssal sinking at high latitudes in what is called the ocean overturning circulation. We derived the ocean area-averaged to illustrate how this circulation sets the vertical distribution of density of the global ocean. This step concluded a *tour de force* of ocean physics from centimeter scales to thousands of kilometers.

References

[1] K. L. Polzin, and J. M. Toole, J. R. Ledwell, R. W. Schmitt, *Spatial Variability of Turbulent Mixing in the Abyssal Ocean*, Science **276**, (1997), 93–96.

[2] L. St. Laurent, and A. C. Naveira Garabato, J. R. Ledwell, A. M. Thurnherr, J. M. Toole, and A. J. Watson, *Turbulence and Diapycnal Mixing in Drake Passage*, Journal of Physical Oceanography **42**, (2012), 2143–2152.

[3] B. L. Wynne-Cattanach, N. Couto, H. F. Drake,. et al, *Observations of diapycnal upwelling within a sloping submarine canyon*, Nature **630** (2024), 884–890.

[4] A. C. Naveira Garabato, C. P. Spingys, B. Fernandez Castro, et al., *Convective turbulent mixing drives rapid upwelling along the ocean?s bottom boundary*, Nature Geoscience, under review.

[5] J. W. Miles, *On the stability of heterogeneous shear flows*, J. Fluid Mech. **10** (1961) 496–508.

[6] L. N. Howard, *Note on a paper of John W. Miles*, J. Fluid Mech. **10** (1961) 509–512.

[7] L. D. Talley, G. L. Pickard, W. J. Emory, J. H. Swift, *Descriptive Physical Oceanography*, Elsevier (2011), 564 pages.

Understanding polar stratification in radiative-advective equilibrium

Rodrigo Caballero

(joint work with Timothy Merlis)

The concept of radiative-convective equilibrium (RCE) and its embodiment in a single-column model [2, 3] is a cornerstone of climate science. RCE prevails when the atmosphere is heated from below and atmospheric radiative cooling to space is balanced by upward turbulent fluxes at the surface. In RCE, vigorous convection constrains the atmospheric temperature profile to to roughly follow a moist adiabat. As a result, the atmosphere becomes more strongly stratified in response to positive radiative forcing, yielding a negative lapse-rate feedback.

The opposite limit to RCE is radiative-advective equilibrium (RAE), where diabatic cooling is primarily balanced by lateral energy flux convergence [6, 1]. RAE prevails in the polar regions, especially in winter [4, 5]. Convection is absent in RAE, and the controls on atmospheric temperature structure are less clear. Full climate model simulations show strong destratification and a positive lapse-rate feedback in response to warming, but we lack a robust conceptual picture of how this response arises and how it relates to changes at lower latitudes [7, 8].

Here, we develop a single-column model of RAE and use it to build such a picture. The main novelty in the model is in the way lateral advective heating Q_{adv} is parameterized. We show that a simple relaxation formulation,

$$Q_{adv} = \frac{1}{\tau}(T_e^{in} - T_e),$$

where $T_e = T + L_v C_p^{-1} q$ is the equivalent temperature in the polar column and T_e^{in} is a prescribed midlatitude profile, accurately captures advective heating in observations. Because humidity q is strongly concentrated near the surface, the perturbation T_e^{in} profile is inherently bottom-heavy, and relaxation toward this perturbation yields an overall destratification of the polar atmosphere. In addition, increased upper-tropospheric humidity yields stronger cooling to space at upper levels, further contributing to the overall destratification.

Furthermore, we introduce the concept of a "surface radiator fin", whereby the lower troposphere cools to the surface while the surface cools directly to space via the water vapor window. The functioning of this radiator fin necessitates thermodynamic disequilibrium between the surface and lower atmosphere, manifest as a surface-based inversion of the temperature profile. We show that the expression

$$D = \langle T_e^{in} \rangle - \left(\frac{F_s}{\sigma\,w}\right)^{1/4},$$

where $\langle \cdot \rangle$ is a lower-tropospheric mean, F_s is surface forcing and w is a non-dimensional measure of the spectral width of the water vapor window, qualitatively predicts the change in disequilibrium D and in the intensity of the temperature inversion. In response to global warming, a strong increase in surface forcing and narrowing of the water vapor window overwhelms the increase in inflow temperature, yielding a strong decrease in D and weakening of the inversion. This explains the strong near-surface destratification seen in climate models and in observations.

In summary, we identify three main mechanisms controlling the polar lapse-rate response to warming: relaxation to a bottom-amplified inflow profile; upper-level cooling by water vapor; and weakening of the surface radiator fin leading to reduced surface inversion strength. As it happens, all three mechanisms imply a destratification of the polar atmosphere in response to global warming.

REFERENCES

[1] T. W. Cronin and M. F. Jansen. *Analytic radiative-advective equilibrium as a model for high-latitude climate.* Geophys. Res. Lett., **43** 449–457, 2016.
[2] S. Manabe and R. F. Strickler. *Thermal equilibrium of the atmosphere with a convective adjustment.* J. Atmos. Sci., **21** 361–385, 1964.
[3] S. Manabe and R. T. Wetherald. *Thermal Equilibrium of the Atmosphere with a Given Distribution of Relative Humidity.* J. Atmos. Sci., **24** 241–259, 1967.
[4] O. Miyawaki, T. A. Shaw, and M. F. Jansen. *Quantifying energy balance regimes in the modern climate, their link to lapse rate regimes, and their response to warming.* J. Climate, **35** 1045–1061, 2022.
[5] O. Miyawaki, T. A. Shaw, and M. F. Jansen. *The emergence of a new wintertime Arctic energy balance regime.* Environ. Res.: Climate, **2** 031003, 2023.

[6] A. E. Payne, M. F. Jansen, and T. W. Cronin. *Conceptual model analysis of the influence of temperature feedbacks on polar amplification.* Geophys. Res. Lett., **42** 9561–9570, 2015.

[7] M. Previdi, K. L. Smith, and L. M. Polvani. *Arctic amplification of climate change: a review of underlying mechanisms.* Environ. Res. Lett., **16** 093003, 2021.

[8] P. C. Taylor, R. C. Boeke, L. N. Boisvert, N. Feldl, M. Henry, Y. Huang, P. L. Langen, W. Liu, F. Pithan, S. A. Sejas, and I. Tan. *Process drivers, inter-model spread, and the path forward: A review of amplified Arctic warming.* Front. Earth Sci., **9** 758361, 2022.

Reporter: Daniel Bäumer

Participants

Dr. Dallas Albritton
Department of Mathematics
University of Wisconsin-Madison
480 Lincoln Drive
Madison, WI 53706-1388
UNITED STATES

Prof. Dr. Amit Apte
Department of Data Science
Indian Institute of Science Education
and Research (IISER)
Dr. Homi Bhabba Road
Pune 411008
INDIA

Daniel Bäumer
Fakultät für Mathematik
Universität Wien
Oskar-Morgenstern-Platz 1
1090 Wien
AUSTRIA

Prof. Dr. Didier Bresch
Laboratoire de Mathématiques
UMR5127 CNRS
Université de Savoie Mont-Blanc
73376 Le Bourget-du-Lac Cedex
FRANCE

Prof. Dr. Oliver Bühler
Center for Atmosphere Ocean Science
Courant Institute of Mathematical
Sciences
New York University
251 Mercer Street
New York, NY 10012-1110
UNITED STATES

Dr. Rodrigo Caballero
Stockholm University
10691 Stockholm
SWEDEN

Prof. Dr. Jörn Callies
Caltech
1200 E. California Blvd.
P.O. Box MC 131-24
Pasadena, CA 91125
UNITED STATES

Prof. Dr. Paola Cessi
Scripps Institution of Oceanography
University of California, San Diego
9500 Gilman Drive
La Jolla, CA 92093-0213
UNITED STATES

Prof. Dr. Colin Cotter
Department of Mathematics
Imperial College London
South Kensington Campus
London SW7 2AZ
UNITED KINGDOM

Prof. Dr. George C. Craig
Lehrstuhl für Theoretische Meteorologie
Ludwig-Maximilians-Universität
Theresienstraße 37
80333 München
GERMANY

Dr. Tom Dörffel
Weierstrass Institute for Applied
Analysis and Stochastics
Mohrenstraße 39
10117 Berlin
GERMANY

Prof. Dr. Eduard Feireisl
Institute of Mathematics of the AS CR
Charles University
Žitná 25
115 67 Praha 1
CZECH REPUBLIC

Dr. Raffaele Ferrari
Department of Earth, Atmospheric
and Planetary Sciences
Massachusetts Institute of Technology
77 Massachusetts Avenue
Cambridge, MA 02139
UNITED STATES

Dr. Anna Frishman
Department of Physics
Technion – Israel Institute of
Technology
Haifa 32000
ISRAEL

Dr. Franziska Glassmeier
Delft University of Technology
Faculty of Civil Engineering and
Geosciences
Department Geoscience and Remote
Sensing
P.O. Box 5048
2600 GA Delft
NETHERLANDS

Prof. Dr. Georg A. Gottwald
School of Mathematics and Statistics
The University of Sydney
Sydney 2206
AUSTRALIA

Prof. Dr. Martin Hairer
Mathematics, EPFL
EPFL SB MATH PROPDE
Station 8
1015 Lausanne
SWITZERLAND

Prof. Peter H. Haynes
Department of Applied Mathematics
and Theoretical Physics (DAMTP)
Centre for Mathematical Sciences
Wilberforce Road
Cambridge CB3 0WA
UNITED KINGDOM

Prof. Dr. Matthias Hieber
Fachbereich Mathematik
Technische Universität Darmstadt
Schloßgartenstraße 7
64289 Darmstadt
GERMANY

Dr. Malte Jansen
Department of the Geophysical Sciences
The University of Chicago
5734 S. Ellis Avenue
Chicago, IL 60637
UNITED STATES

Dr. Yohai Kaspi
Department of Earth and Planetary
Sciences
Weizmann Institute of Science
234 Herzl st.
Rehovot 76 00
ISRAEL

Prof. Dr. Rupert Klein
Fachbereich Mathematik und Informatik
Freie Universität Berlin
Arnimallee 6
14195 Berlin
GERMANY

Prof. Dr. Peter Korn
Max Planck Institute for Meteorology,
Hamburg
Bundesstraße 55
20146 Hamburg
GERMANY

Prof. Dr. Jinkai Li
South China Research Center of Applied
Mathematics and Interdisciplinary
Studies
School of Mathematical Sciences
South China Normal University
No. 55, Zhongshan Avenue West
Guangzhou 510631
CHINA

Dr. Simon Markfelder
Institut für Mathematik
Universität Würzburg
Emil-Fischer-Straße 40
97074 Würzburg
GERMANY

Prof. Dr. Stephan Pfahl
Institut für Meteorologie
Freie Universität Berlin
Carl-Heinrich-Becker-Weg 6-10
12165 Berlin
GERMANY

Dr. Annette Rudolph
FG KI und Landnutzungswandel
Technische Universität Berlin
Straße des 17. Juni 145
10623 Berlin
GERMANY

Dr. Lisa Schielicke
Meteorologie
Universität Bonn
Auf dem Hügel 20
53121 Bonn
GERMANY

Dr. Axel Seifert
Deutscher Wetterdienst
Frankfurter Straße 135
63067 Offenbach am Main
GERMANY

Dr. Tiffany Shaw
419 Henry Hinds Laboratory for the
Geophysical Sciences
The University of Chicago
5734 South Ellis Avenue
Chicago, IL 60637-1433
UNITED STATES

Prof. Dr. Pier Siebesma
Department Geoscience and Remote
Sensing
Delft University of Technology
P. O. Box 5031
2600 GA Delft
NETHERLANDS

Dr. Martin Singh
Earth, Atmosphere & Environment
Monash University
9 Rainforest Walk
Clayton, Victoria 3168
AUSTRALIA

Prof. Dr. Samuel N. Stechmann
Department of Mathematics
University of Wisconsin-Madison
480 Lincoln Drive
Madison, WI 53706-1388
UNITED STATES

Prof. Dr. Bjorn Stevens
Max-Planck-Institut für
Meteorologie
Universität Hamburg
Bundesstr. 53
20146 Hamburg
GERMANY

Prof. Dr. Edriss S. Titi
Department of Applied Mathematics and
Theoretical Physics
Centre for Mathematical Sciences
University of Cambridge
Wilberforce Road
Cambridge CB3 0WA
UNITED KINGDOM

Dr. Eli Tziperman
Department of Earth and Planetary
Sciences
Harvard University
20 Oxford Street
Cambridge, MA 02138
UNITED STATES

Prof. Dr. Geoffrey K. Vallis
Department of Mathematics
University of Exeter
North Park Road
Exeter EX4 4QE
UNITED KINGDOM

Prof. Dr. Jacques Vanneste
School of Mathematics
University of Edinburgh
James Clerk Maxwell Bldg.
King's Buildings, Peter G Tait Road
Edinburgh EH9 3FD
UNITED KINGDOM

Prof. Dr. Nikki Vercauteren
Institute of Geophysics and Meteorology
University of Cologne
50969 Köln
GERMANY

Jan Wachtendonk
Fachbereich Mathematik & Informatik
Freie Universität Berlin
Arnimallee 9
14195 Berlin
GERMANY

Prof. Dr. William R. Young
Scripps Institution for Oceanography
University of California, San Diego
9500 Gilman Drive
La Jolla CA 92093-0209
UNITED STATES

Dr. Yeyu Zhang
Shanghai University of Finance and
Economics
777 Guoding Road
200433 Shanghai Shi
CHINA